JOURNAL INDIAN ASSOCIATION OF SEDIMENTOLOGISTS ISSN NO: 2582 - 2020
Vol. 37, Issue 2, 2020, pp. 61-90
DOI: http://dx.doi.org/10.51710/jias.v37i2.117

Gravity flows: Types, definitions, origins, identification markers, and problems

G. Shanmugam
Department of Earth and Environmental Sciences, The University of Texas at Arlington,
Arlington, TX 76019, USA
E-mail: shanshanmugam@aol.com

Abstract

This review covers 135 years of research on gravity flows since the first reporting of density plumes in the Lake Geneva, Switzerland by Forel (1885). Six basic types of gravity flows have been identified in subaerial and suaqueous environments. They are: (1) hyperpycnal flows, (2) turbidity currents, (3) debris flows, (4) liquefied/fluidized flows, (5) grain flows, and (6) thermohaline contour currents. The first five types are flows in which the density is caused by sediment in the flow, whereas in the sixth type, the density is caused by variations in temperature and salinity. Although all six types originate initially as downslope gravity flows, only the first five types are truly downslope processes, whereas the sixth type eventually becomes an alongslope process. (1) Hyperpycnal flows are triggered by river floods in which density of incoming river water is greater than the basin water. These flows are confined to proximity of the shoreline. They transport mud, and they do not transport sand into the deep sea. There are no sedimentological criteria yet to identify hyperpycnites in the ancient sedimentary record. (2) A turbidity current is a sediment-gravity flow with Newtonian rheology and turbulent state in which sediment is supported by flow turbulence and from which deposition occurs through suspension settling. Typical turbidity currents can function as truly turbulent suspensions only when their sediment concentration by volume is below 9% or C < 9%. This requirement firmly excludes the existence of 'high-density turbidity currents'. Turbidites are recognized by their distinct normal grading in deep-water deposits. (3) A debris flow (c. 25-100%) is a sediment-gravity flow with plastic rheology and laminar state from which deposition occurs through freezing *en masse*. The terms debris flow and mass flow are used interchangeably. General characteristics of muddy and sandy debrites are floating clasts, planar clast fabric, inverse grading, etc. Most sandy deep-water deposits are sandy debrites and they comprise important petroleum reservoirs worldwide. (4) A liquefied/fluidized flow (>25%) is a sediment-gravity flow in which sediment is supported by upward-moving intergranular fluid. They are commonly triggered by seismicity. Water-escape structures, dish and pillar structures, and SSDS are common. (5) A grain flow (c. 50-100%) is a sediment-gravity flow in which grains are supported by dispersive pressure caused by grain collision. These flows are common on the slip face of aeolian dunes. Massive sand and inverse grading are potential identification markers. (6) Thermohaline contour currents originate in the Antarctic region due to shelf freezing and the related increase in the density of cold saline (i.e., thermohaline) water. Although they begin their journey as downslope gravity flows, they eventually flow alongslope as contour currents. Hybridites are deposits that result from intersection of downslope gravity flows and alongslope contour currents. Hybridites mimic the "Bouma Sequence" with traction structures (Tb and Tc). Facies models of hyperpycnites, turbidites, and contourites are obsolete. Of the six types of density flows, hyperpycnal flows and their deposits are the least understood.

Keywords: Debris flow, Gravity flow, Fluidized/Liquefied flow, Grain flow, Hyperpycnal flow, Thermohaline contour current, Turbidity current

Introduction

Gravity flows are the most consequential sedimentary phenomena in the geologic record. From a sedimentological perspective, density flows are ubiquitous in both subaerial and suaqueous environments. Importantly, gravity flows dominate in shelf, slope, and basin environments. They are caused not only by sediment density, but also by changes in temperature and salinity. Furthermore, density flows travel not only downslope, but also alongslope. Therefore, the key objectives of this article are (1) to identify and discuss basic types of density flows, (2) to provide a clear definition of each flow type, (3) to identify their origins or triggering mechanisms, (4) to suggest identification markers of their deposits, and (5) to identify the remaining unresolved problems in aiding future research. I have attempted to accomplish these objectives by integrating:

1) theoretical considerations,
2) experimental verifications,
3) modern submarine observations,
4) modern subaerial observations,
5) ancient outcrop examples, and
6) modern and ancient subsurface (sediment core) examples.

I have selected the following six basic types of density flows for discussion in this review (Table 1). The density value cited for each example is to provide a relative sense, and they should not be considered typical of the example.

Table 1. Six types of gravity (density) flows and their characteristics.

Flow type	Flow attributes	Environment	Origins (Triggers)	Reliability of identification markers
1. Hyperpycnal flow	Density of river water > Density of basin water SSC (Suspended sediment concentration) (ρ): 0.025 g/cm^3 (Wright and Nittrouer, 1995)	Subaqueous only, near shoreline	River floods	Unreliable facies model because of absence of modern sediment core and experimental observations (Shanmugam, 2018a)
2. Turbidity current	Newtonian rheology Turbulent state C < 9% by volume (Bagnold, 1962) Flow density (ρ): 1.1 g/cm^3 (Kuenen, 1966) Deposition by settling	Subaqueous only, shelf, slope, and basin	Earthquake, slope instability, oversupply of sediment, volcanism, meteorite impact, tsunamis, cyclones	Reliable normal grading
3. Debris flow	Plastic rheology Laminar state C: 25-100% Flow density (ρ): 2 g/cm^3 (Hampton, 1972) En masse freezing	Subaerial and subaqueous	Earthquake, slope instability, oversupply of sediment, volcanism, meteorite impact, tsunamis, cyclones	Reliable markers because of modern examples and experimental observations (Shanmugam, 2000; Marr et al., 2001)
4. Liquefied/Fluidized flow	Upward moving fluid Flow density (ρ): 1.8 g/cm^3 (Breien et al., 2010)	Subaerial and Subaqueous	Earthquakes, volcanism, meteorite impacts, tsunamis, cyclones,	Reliable markers because of modern examples in earthquake-induced SSDS (Shanmugam, 2017)
5. Grain flow	Frictional strength Grain collision (Dispersive pressure) Flow (ρ): 2.1—2.3 g/ cm^3 (Parsons et al.,, 2001)	Subaerial and subaqueous, aeolian dunes and submarine canyons	Climate, wind, steep gradients	Reliable markers because of modern examples in aeolian dunes and in submarine canyons

6. Thermohaline contour current (THCC)	Current reworking Antarctic Bottom Water (AABW) density (ρ): 0.03 g/cm^3 (Purkey et al., 2018) Bottom Water density in Ross Sea, Antarctica at 4,000 m water depth (ρ): 0.03 g/cm^3 (Henze, 2015, her Fig. 2.14)	Subaqueous only, shelf edge, slope, basin.	Shelf freezing (Temperature and salinity) in Antarctica. Note that THCC began as downslope gravity flows (Fig. 36), but became a contour current.	Reliable markers because of modern sediment cores (Hollister, 1967)

This review should be helpful from both an academic and an applied point of view. For example, identification markers of deposits of density flows are of practical value because sandy debrites and associated mass-transport deposits are important petroleum reservoirs in the North Sea (Shanmugam et al., 1995), Nigeria (Shanmugam, 2012), Bay of Bengal (Shanmugam et al., 2009), Gulf of Mexico, Russia and Australia (Meckel, 2010; Meckel et al. 2011) and China (Zou et al., 2012). Global economic significance of sandy contourites has been discussed by Viana (2008), Stow et al. (2011), and Shanmugam (2017c). In terms of regional importance, Mullins et al. (1980) discussed carbonate sandy contourites in the Straits of Florida, and Shanmugam et al. (1993) documented measured porosity and permeability values of petroleum-producing sandy contourites in the Ewing Bank area of the Gulf of Mexico.

Gravity flows

The term “gravity flow” is used here for a continuous, irreversible deformation of sediment-water mixture that occurs in response to applied shear stress, which is gravity in most cases (Pierson and Costa 1987, p. 2). In this article, density flows and gravity flows are considered to be one and the same, although density represents mass per unit volume and gravity represents a force. Gravity flows have been of great interest to sedimentologists and engineers for over 100 years, since the first discussion of theory of turbulence in fluid mechanics (Prandtl, 1925, 1926). Selected publications on this domain are of Kuenen (1951 and 1953), Bates (1953), Bagnold (1954 and 1962), Dott (1963), Sanders (1965), Middleton (1965, 1966, 1967, 1970, 1993), Klein (1966 and 1975), Middleton and Bouma (1973), Hampton (1972), Middleton and Hampton (1973), Lowe (1976a, 1976b, 1982), Kneller (1995), Shanmugam 1996, 2000, 2002, 2006, 2012, 2015, 2018a, b, 2019a, b), Iverson (1997), Rebesco et al. (2008), and Zenk (2008).

Gravity-driven downslope processes

Because all six types begin their journey as downslope gravity flows, some basic principles are briefly discussed here on gravity-driven downslope processes.

Mass transport and turbidity currents

Dott (1963) proposed the most meaningful and practical classification of subaqueous mass-transport processes. In this scheme, subaqueous processes are broadly classified into (1) elastic, (2) elastic and plastic, (3) plastic, and (4) viscous fluid types based on mechanical behavior (Fig. 1). The elastic behavior represents rockfall; the elastic and plastic behavior comprises slide and slump; the plastic behavior represents debris flow; and the viscous fluid represents Newtonian turbidity current. The importance of Dott’s (1963) classification is that mass-transport processes do not include turbidity currents (Fig. 1C). In this article, although mass-transport processes are composed of three basic types: (1) slide, (2) slump, and (3) debris flow (Fig. 1), only debris flow is considered as a 'flow'. The reason is that slides and slumps are coherent masses and they are not composed of sediment-water mixtures, a condition that is a prerequisite in defining a 'flow'.

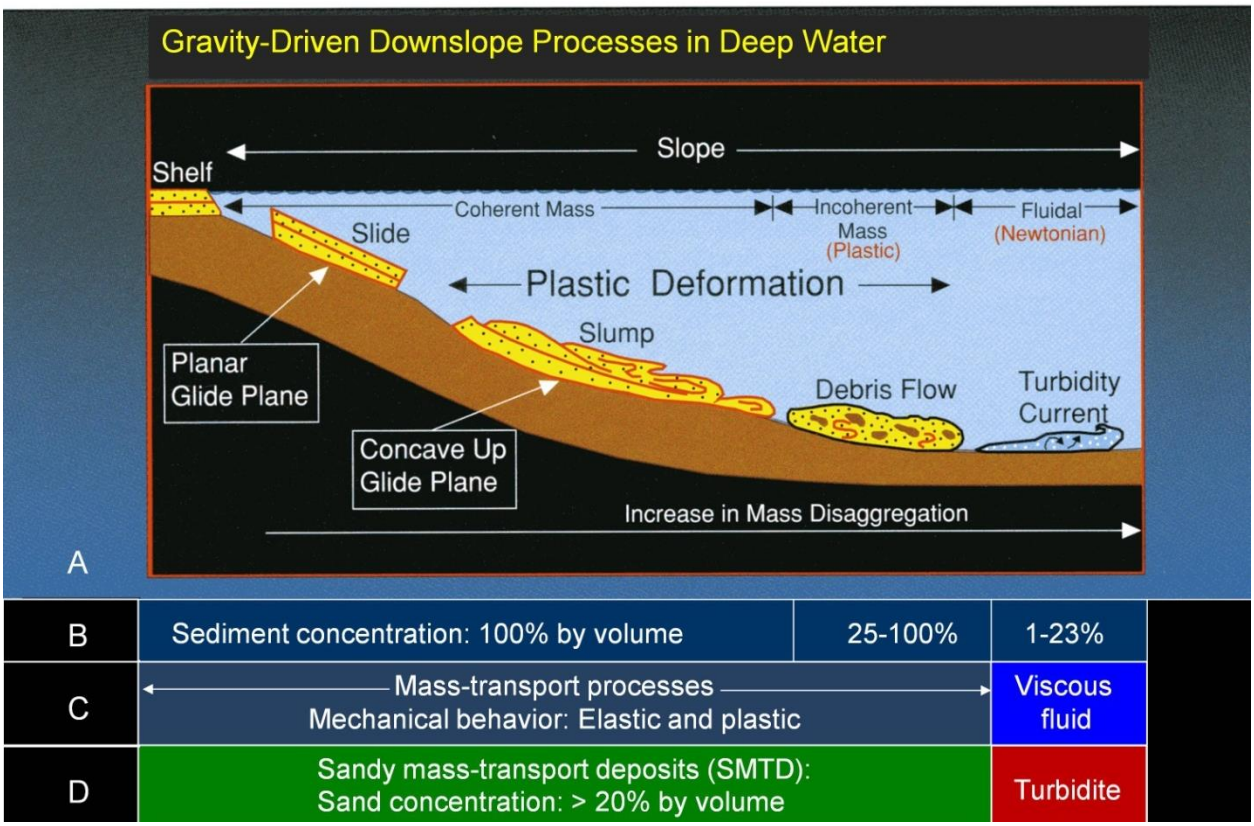

Fig. 1. (A) Schematic diagram showing four common types of gravity-driven downslope processes that transport sediment into deep-marine environments. A slide represents a coherent translational mass transport of a block or strata on a planar glide plane (shear surface) without internal deformation. A slide may be transformed into a slump, which represents a coherent rotational mass transport of a block or strata on a concave-up glide plane (shear surface) with internal deformation. Upon addition of fluid during downslope movement, slumped material may transform into a debris flow, which transports sediment as an incoherent body in which intergranular movements predominate over shear-surface movements. A debris flow behaves as a plastic laminar flow with strength. As fluid content increases in debris flow, the flow may evolve into Newtonian turbidity current. Not all turbidity currents, however, evolve from debris flows. Some turbidity currents may evolve directly from sediment failures. Turbidity currents can develop near the shelf edge, on the slope, or in distal basinal settings. (B) Sediment concentration (% by volume) in gravity-driven processes. Slides and slumps are composed entirely of sediment (100% by volume). Debris flows show a range of sediment concentration from 25% to 100% by volume. Note that turbidity currents are low in sediment concentration (1%–23% by volume), implying low-density flows. These values are based on published data (see Shanmugam, 2000, his Fig. 4). (C) Based on mechanical behavior of gravity-driven downslope processes, mass-transport processes include slide, slump, and debris flow, but not turbidity currents (Dott, 1963). (D) The prefix "sandy" is used for mass-transport deposits (SMTDs) that have grain (> 0.06 mm: sand and gravel) concentration value equal to or above 20% by volume. The 20% value is adopted from the original field classification of sedimentary rocks by Krynine (1948). (A) Reproduced from Shanmugam et al. (1994).

The underpinning principle of Dott's (1963) classification is the separation of solid from fluid mode of transport based on sediment concentration. In the solid (elastic and plastic) mode of transport, high sediment concentration is the norm (25-100% by volume, Fig. 1B). Mass-transport mechanisms are characterized by solid blocks or aggregate of particles (mass). In contrast, individual particles are held in suspension by fluid turbulence in turbidity currents (Dott, 1963; Sanders, 1965). Turbidity currents are characterized by low sediment concentration (Bagnold, 1962).

Mass transport can operate in both subaerial and subaqueous environments, but turbidity current can operate only in subaqueous environments. The advantage of this classification is that physical features preserved in a deposit directly represent the physics of

sediment movement that existed at the final moments of deposition. The link between the deposit and the physics of the depositional process can be established by practicing the principle of process sedimentology, which is detailed bed-by-bed description of sedimentary rocks and their process interpretation (Shanmugam, 2006).

Sediment-gravity flows

Middleton and Hampton (1973) distinguished sediment-gravity flows from fluid gravity flows. In a *fluid-gravity flow* (e.g., river currents and some deep-ocean currents), fluid is directly driven by gravity, whereas in a *sediment-gravity flow* the interstitial fluid is driven by the grains moving downslope under the influence of gravity. Furthermore, Middleton and Hampton classified sediment-gravity flows into four types based on sediment-support mechanisms (Fig. 2). They are: (1) *turbidity current* with turbulence; (2) *fluidized sediment flow* with upward moving intergranular flow; (3) *grain flow* with grain interaction (i.e., dispersive pressure); and (4) *debris flow* with matrix strength. Sandy debris flows occupy an intermediate region between debris flows and grain flows (Fig. 2).

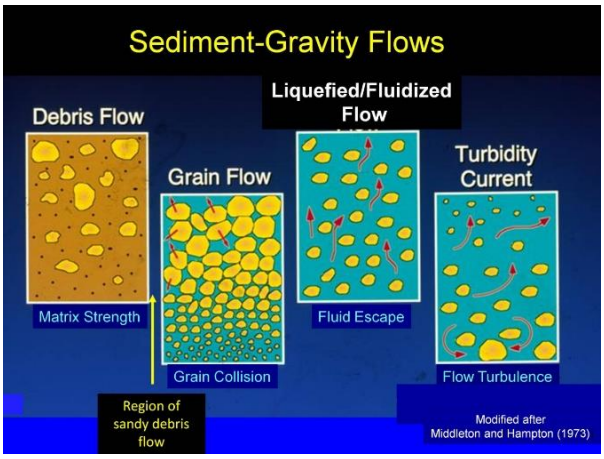

Fig. 2. Classification of sediment-gravity flows based on sediment-support mechanisms by Middleton and Hampton (1973). The position of sandy debris flow is shown for comparison.

Newtonian vs. plastic fluid rheology

In this article, the focus is on debris flows and turbidity currents because of their importance. These two processes are distinguished from one another on the basis of fluid rheology and flow state. The rheology of fluids can be expressed as a relationship between applied shear stress and rate of shear strain (Fig. 3). Newtonian fluids (i.e., fluids with no inherent strength), like water, will begin to deform the moment shear stress is applied, and the deformation is linear. In contrast, some naturally occurring materials (i.e., fluids with strength) will not deform until their yield stress has been exceeded (Fig. 3); once their yield stress is exceeded, deformation is linear. Such materials (e.g., wet concrete) with strength are considered to be Bingham plastics (Fig. 3). For flows that exhibit plastic rheology, the term plastic flow is appropriate. Using rheology as the basis, deep-water sediment flows are divided into two broad groups, namely, (1) Newtonian flows that represent turbidity currents and (2) plastic flows that represent debris flows.

Turbulent vs. laminar flow state

In addition to fluid rheology, flow state is used in distinguishing laminar debris flows from turbulent turbidity currents. The difference between laminar and turbulent flows was demonstrated in 1883 by Osborne Reynolds, an Irish engineer, by injecting a thin stream of dye into the flow of water through a glass tube. At low rates of flow, the dye stream traveled in a straight

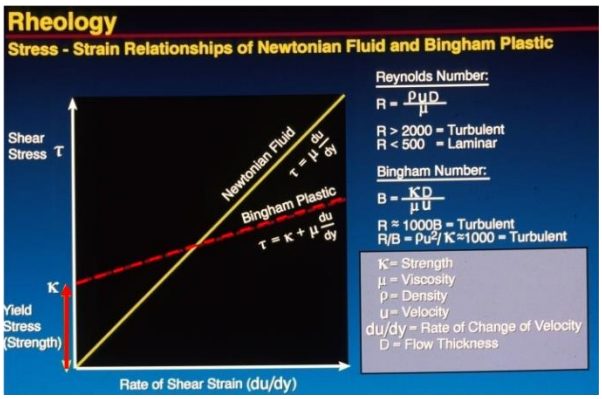

Fig. 3. Rheology (stress-strain relationships) of Newtonian fluids and Bingham plastics. Graph shows that the fundamental rheological difference between debris flows (Bingham plastics) and turbidity currents (Newtonian fluids) is that debris flows exhibit strength, whereas turbidity currents do not. Reynolds number is used for determining whether a flow is turbulent (turbidity current) or laminar (debris flow) in state. Compiled from several sources (Dott, 1963; Enos, 1977; Pierson and Costa, 1987; Phillips and Davies, 1991; Middleton and Wilcock, 1994). After Shanmugam (1997).

path. This regular motion of fluid in parallel layers, without macroscopic mixing across the layers, is called a laminar flow. At higher flow rates, the dye stream broke up into chaotic eddies. Such an irregular fluid motion, with macroscopic mixing across the layers, is called a turbulent flow. The change from laminar to turbulent flow occurs at a critical Reynolds number (the

ratio between inertia and viscous forces) of about 2000 (Fig. 4).

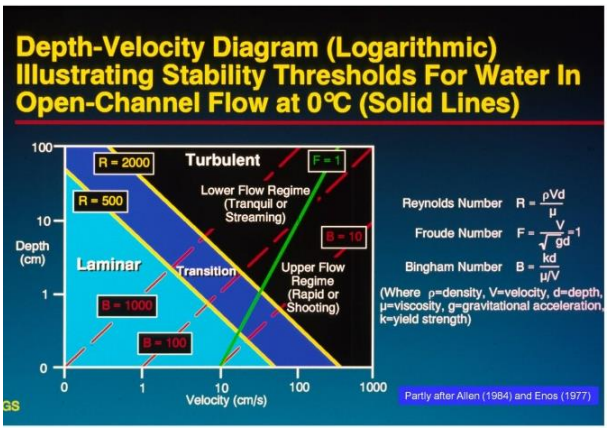

Fig. 4. Depth-velocity diagram showing laminar and turbulent fields of fluids. Partly after Allen (1984) and Enos (1977).

Sediment concentration

Sediment concentration is the most important property in controlling fluid rheology (Fig. 5). Classification of gravity-driven sediment flows into Newtonian and plastic types is based on fluid rheology. Turbidity currents are Newtonian flows, whereas all mass flows (muddy debris flows, sandy debris flows, and grain flows) are plastic flows. Turbidity currents occur only as subaqueous flows, whereas debris flows and grain flows can occur both as subaerial and as subaqueous flows. High-density turbidity currents are not meaningful in this rheological classification because their sediment concentration values represent both Newtonian and plastic flows (see Shanmugam, 1996).

In the following discussion, each density flow is evaluated with the above principles in mind.

Hyperpycnal flows

Definition

Forel (1885, 1892) first reported the phenomenon of density plumes in the Lake Geneva (Loc. Léman), Switzerland. In advocating a rational theory for delta formation, Bates (1953) suggested three types: (1) hypopycnal plume for floating river water that has lower density than basin water (Fig. 6a); (2) homopycnal plume for mixing river water that has equal density as basin water (Fig. 6b); and (3) hyperpycnal plume for sinking river water that has higher density than basin water (Fig. 6c). A. plume is a

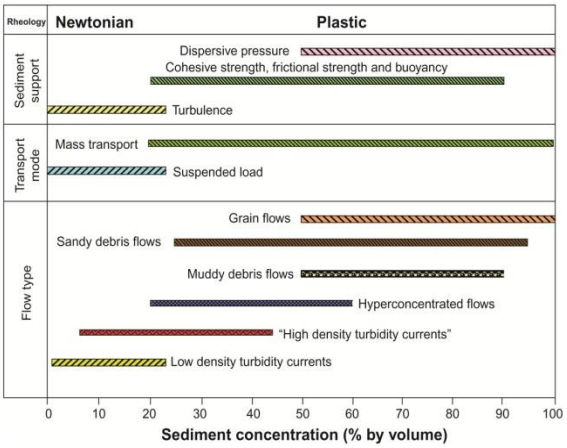

Fig. 5. Classification of gravity-driven sediment flows, based on sediment concentration, into Newtonian and plastic types. Sediment concentration is the most important property in controlling fluid rheology. High-density turbidity currents are included here solely for purposes of discussion. Also, for purposes of comparison, subaerial flows (river currents and hyper-concentrated flows) are considered. Published values of sediment concentration by volume percent are: (1) river currents (1-5%; e.g., Galay, 1987), (2) low-density turbidity currents (1-23%; e.g., Middleton, 1967, 1993), (3) high-density turbidity currents (6-44%; Kuenen, 1966; Middleton, 1967), (4) hyper-concentrated flows (20=60%; Pierson and Costa, 1987), (5) muddy debris flows (50-90%; Coussot and Muenier, 1996), (6) sandy debris flows (25-95%; Shanmugam, 1997; which was partly based on reinterpretations of various processes that exhibit plastic rheology in papers by Middleton, 1966, 1967; Wallis, 1969; Lowe, 1982; Shultz, 1984), (7) grain flows (50-100%; partly based on Rodine and Johnson, 1976; Shultz, 1984; Pierson and Costa, 1987). After Shanmugam (2000). Reproduced with permission from Elsevier.

fluid enriched in sediment, ash, biological or chemical matter that enters another fluid. However, the term "flow" is used for a continuous, irreversible deformation of sediment-water mixture that occurs in response to applied shear stress, which is gravity in most cases (Pierson and Costa 1987, p. 2). Not all plumes are flows. For example, floating hypopycnal plumes are not driven by gravity (Fig. 6a). However, both terms "flow" and "plume" are applicable to hyperpycnal type. This is because hyperpycnal type behaves as bed load due to higher sediment concentration (Fig. 6C).The other practice is to employ terms "overflow", "interflow", and "underflow" for hypopycnal, homopycnal, and hyperpycnal plumes, respectively. Again, the term flow is not appropriate for hypopycnal plume that is unaffected by gravity.

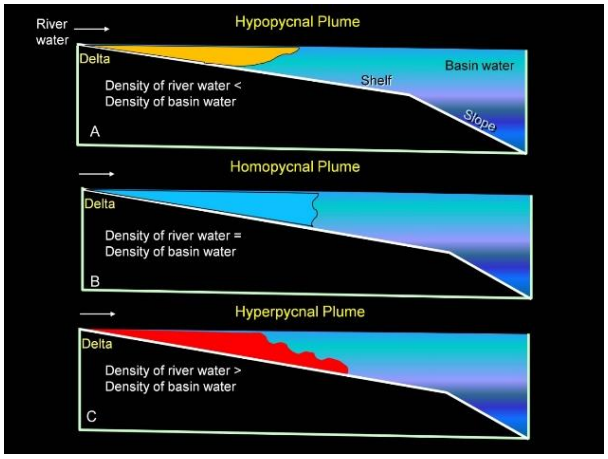

Fig. 6. Concepts and examples of density plumes. a, b, and c Schematic diagrams showing three types of density variations in riverine plumes in deltaic environments based on concepts of Bates (1953). Figure from Shanmugam (2012) with permission from Elsevier

Origin

Hyperpycnal flows originate from river floods at the plunge points near the shoreline. Mulder et al. (2003) expanded the applicability of the concept of hyperpycnal plumes from shallow water (deltaic) to deep-water (continental slope and abyssal plain) environments. In this new development, hyperpycnal flows are considered analogous to turbidity currents in many respects (Mulder et al., 2003; Steel et al., 2016; Zavala and Arcuri, 2016).

It is worth noting that Middleton and Hampton (1973) did not consider hyperpycnal flows in their original classification of sediment-gravity flows (Fig. 2), although hyperpycnal flows are indeed driven by sediment gravity. For the following reasons, hyperpycnal flows are considered as sediment-gravity flows in this article.

1. River-mouth hyperpycnal flows are caused by higher density of the entering river flows in comparison to density of seawater (Bates, 1953). Sediment particles in the flow are the cause of higher flow density.
2. The other option for higher density of entering flow is by changes in salinity and/or temperature, such as thermohaline ocean-bottom contour currents (Gordon, 2019), which is unlikely to occur at river mouths.
3. By applying the concept of Middleton and Hampton (1973), where the river waters enter the ocean, density of ambient fluid changes from air (1.225 kg/ m^{-3}) to seawater (1030 kg/m^{-3}) (Beicher, 2000). In other words, at river-mouth plunge points, fluid-gravity flows could transform into sediment-gravity flows (Fig. 7). However, fluid mechanics of hyperpycnal flows is mired in controversies (Shanmugam, 2018a, 2019b). Importantly, this flow transformation does not imply that all river flows routinely become turbidity currents.

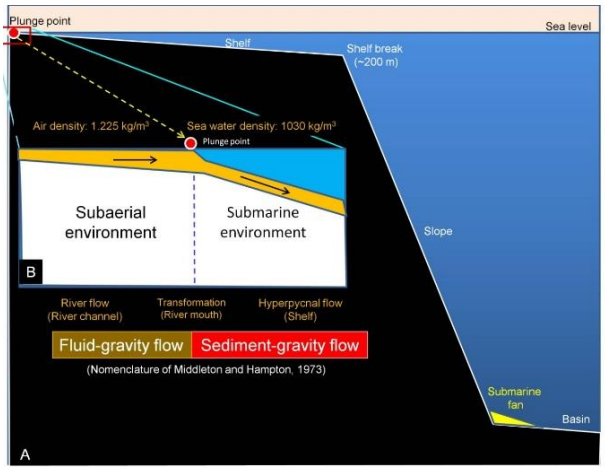

Fig. 7. Conceptual diagram of a continental margin showing relative positions of plunge point (red filled circle) at river mouth and submarine fan at base-of-slope. Note that fluid-gravity flows can transform into sediment-gravity flows at plunge points and deposit sediments as hyperpycnites near the shoreline in shallow-water environments. From Shanmugam (Shanmugam, 2020).

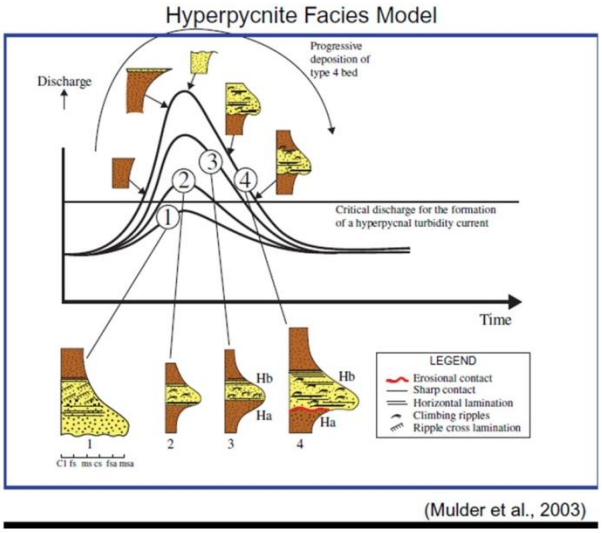

Fig. 8. Hyperpycnite facies model showing inverse to normal grading with erosional contact in the middle. Note identical inverse to normal grading trend in the contourite facies model (Fig. 44). From Mulder et al. (2003)

Identification

- Facies model (Mulder et al., 2003)
- Inverse- to normal- grading (Fig. 8)

- Internal erosion surface (Fig. 8)

Problem

Although there are modern plumes that may be termed hyperpycnal flows (Fig. 9), there are problems associated with recognizing hyperpycnal flows using aerial photographs and satellite images because these images do not provide information on fluid rheology, low state, and sediment concentration in distinguishing hyperpycnal flows from turbidity currents. The basic issue is that hyperpycnal plumes are defined purely based on density (Bates, 1953).

Fig. 9. Sediment plume triggered by Elwha Dam demolition in the State of Washington (USA), (A) Index map showing Elwha Dam (arrow). The 108-foot dam, built in 1910 and demolished in 2012, is located approximately 7.9 km upstream from the river mouth. Credit: U.S. Geological Survey Public Domain map, (B) Aerial photograph of the Olympic Peninsula and the Strait of Juan de Fuca. Note the Elwha River mouth is shown by a filled yellow circle. From Duda et al. (2011) with additional labels by G. Shanmugam, (C) Elwha sediment plume triggered by the demolition of Elwha Dam in 2012. Red arrow shows easterly deflecting plume, away from the Pacific Ocean. This deflection could be attributed to tidal currents in this estuarine environment. Also, the Strait of Juan de Fuca is subjected to easterly upwelling winds. Photo credit: Tom Roorda. Aerial photo was taken on March 30, 2012. From Hickey (2013), UW News, March 7, 2013, University of Washington, Seattle, WA, (D) Aerial photo of Elwha River mouth showing absence of sediment plume in 2019 (compare with Fig. 9C). Photo courtesy of Tom Roorda, Roorda Aerial, Port Angeles, WA. Aerial photo was taken on February 28, 2019.

Although such a definition was adequate in 1953, it is no longer sufficient in light of advances that have been made on fluid dynamics discussed earlier.

Major unresolved problems are:

(1). Facies model has not been reproduced in experiments.

(2). There has not been any verification of inverse to normal grading based on sediment core from modern hyperpycnites.

(3). There are 16 types of hyperpycnal flows, but their fluid dynamical properties have not been verified in experiments. Specifically, deposits of single layer type, double layer type, multi-layer type, etc. (Fig. 10) have not been documented.

(4) The nomenclatural problem is further muddled by classifying turbidity currents and debris flows as "hyperpycnal flows" based on provenance (i.e.,land derived) (Fig. 11) by Zavala (2020). The reason is that debris flows and turbidity currents were traditionally classified as sediment-gravity flows based on sediment-support mechanisms by Middleton and Hampton (1973), which is the standard reference in process sedimentology.

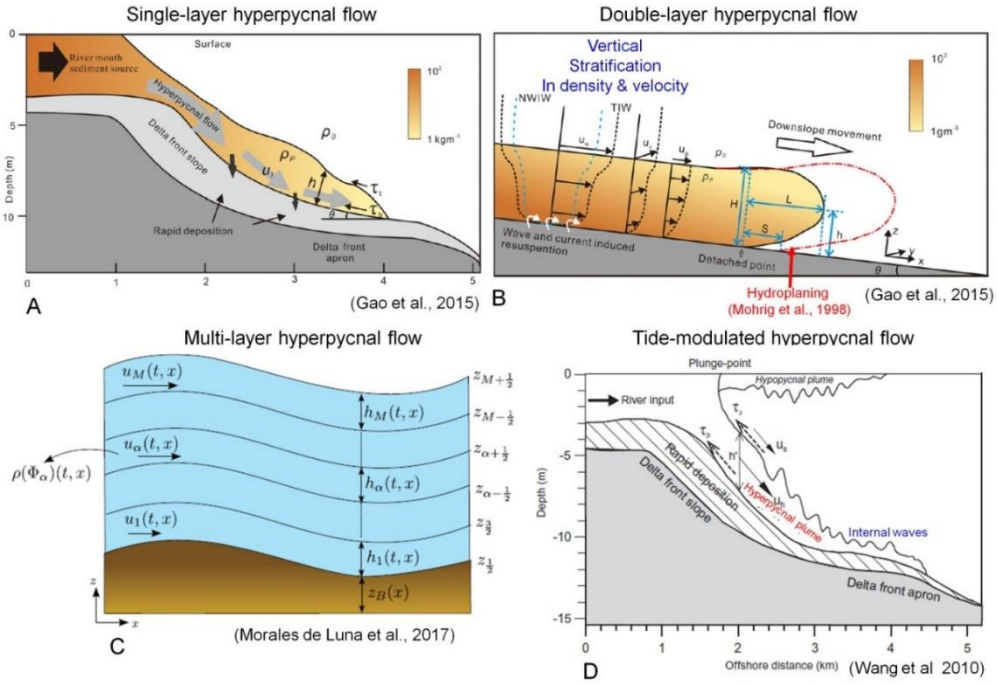

Fig. 10. Four types of hyperpycnal flows. From Shanmugam (2018a). (Correction in reference Wang et al., 2010 in Figure)

(5). Finally, there are 22 external controls (Fig. 12) and their role on deposits of hyperpycnal flows has never been studied.

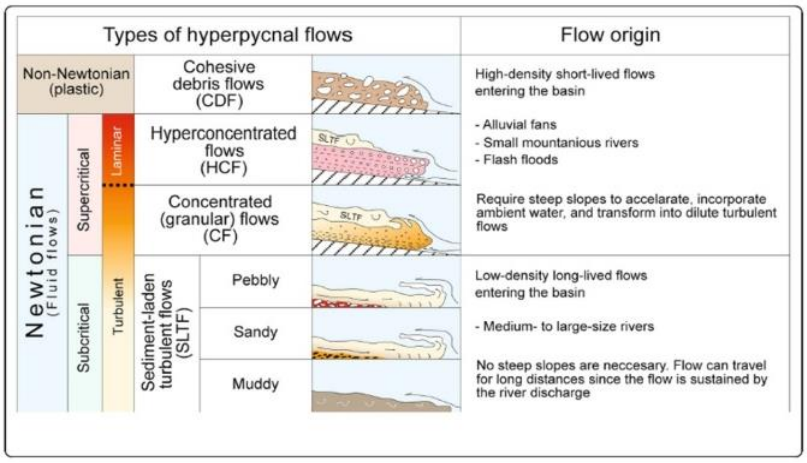

Fig. 11. Classification of debris flows and turbidity currents as "hyperpycnal flows" by Zavala (2020), causing confusion. Note that sediment-gravity flows were originally classified on the basis of sediment-support mechanisms by Middleton and Hampton (1973), whereas Zavala (2020) has classified types of sediment-gravity flows as "hyperpycnal flows" on the basis of their provenance (i.e., land derived). Other problems associated with hyperpycnal flows were addressed by Shanmugam (2018a and 2019b). Figure

Turbidity Currents

Definition

A turbidity current is a sediment flow with Newtonian rheology (Fig. 3) and turbulent state (Figs 13 and 14) in which sediment is supported by turbulence and from which deposition occurs through suspension settling (Dott, 1963; Sanders, 1965; Middleton and Hampton, 1973; Shanmugam, 1996).

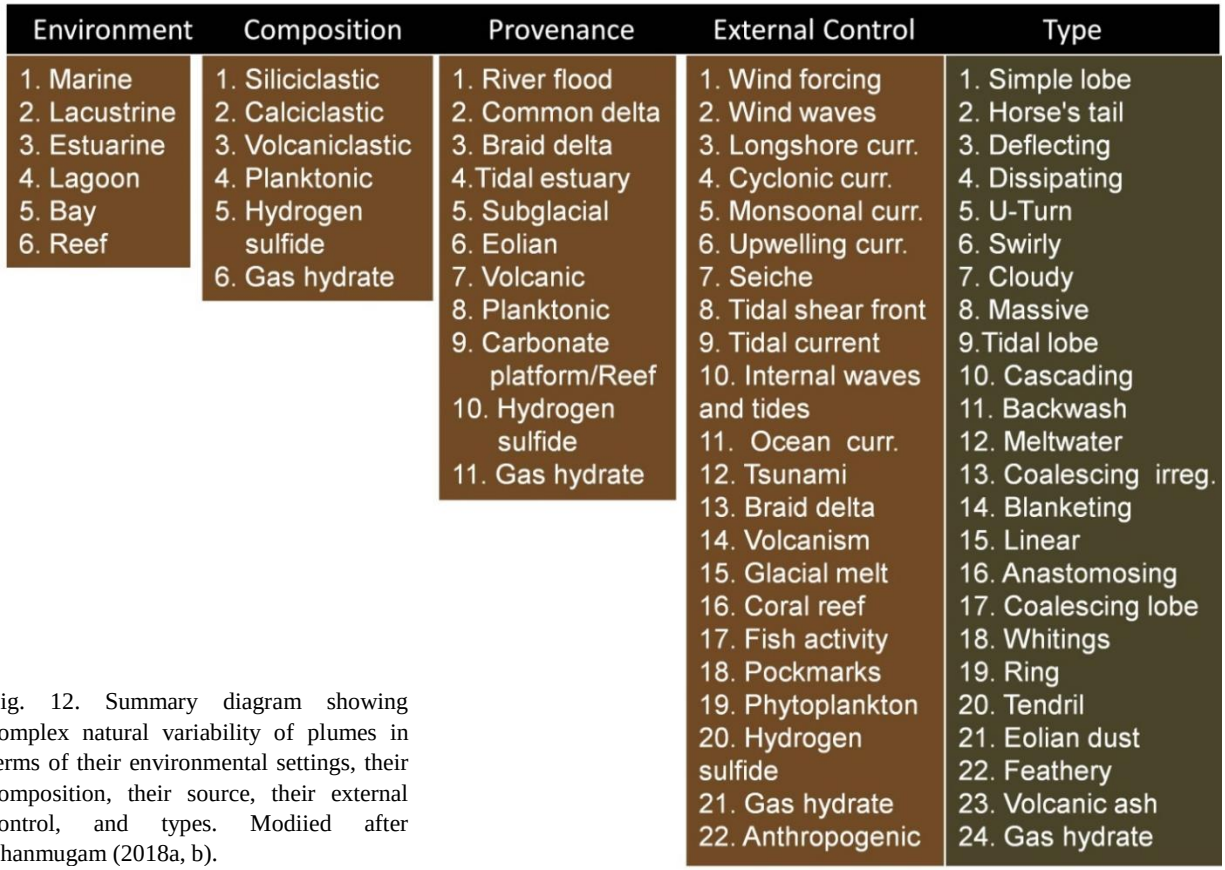

Fig. 12. Summary diagram showing complex natural variability of plumes in terms of their environmental settings, their composition, their source, their external control, and types. Modiied after Shanmugam (2018a, b).

Turbidity currents exhibit unsteady and non-uniform flow behavior (Fig. 13), and they are surge-type waning flows. As they flow downslope, turbidity currents (Fig. 13) invariably entrain ambient fluid (sea water) in their frontal head portion due to turbulent mixing (Allen, 1985). With increasing fluid content, plastic debris flows may tend to become turbidity currents with high turbulence (Fig. 14). However, not all turbidity currents evolve from debris flows. Some turbidity currents may evolve directly from sediment failures. Although turbidity currents may constitute a distal end member in basinal areas, they can occur in any part of the system (i.e., shelf edge, slope, and basin).

Origin (Triggers)

The origins of four sediment-gravity flows are closely related to sediment failures and slope instability. There are 21 triggering mechanisms in causing sediment failures (Shanmugam, 2015), but only important mechanisms are listed in each case.

- Earthquake,
- oversupply of sediment,
- volcanism,
- meteorite impact,
- tsunamis, and
- cyclones

.

Identification Turbidity currents cannot transport gravel and coarse-grained sand in suspension because they do not possess the strength like debris flows. General characteristics of turbidites are:

- Fine-grained sand to mud
- Flute casts as sole marks (Fig. 15). However, bottom currents could also generate such sole marks (core and outcrop), (Klein , 1966).
- Normal grading (core and outcrop) (Fig. 16).
- Sharp or erosional basal contact (core and outcrop) (Fig. 16)
- Gradational upper contact (core and outcrop) (Fig. 16).

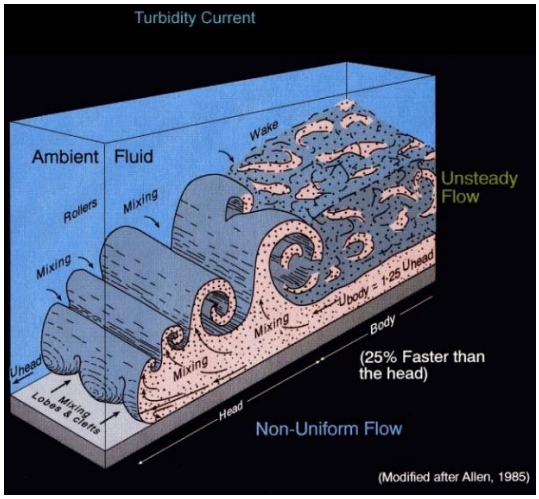

Fig. 13. Photograph of front view of experimental turbidity current showing flow turbulence. Photo from experiments conducted by M. L. Natland and courtesy of G. C. Brown. Published in Shanmugam, G. (2012).

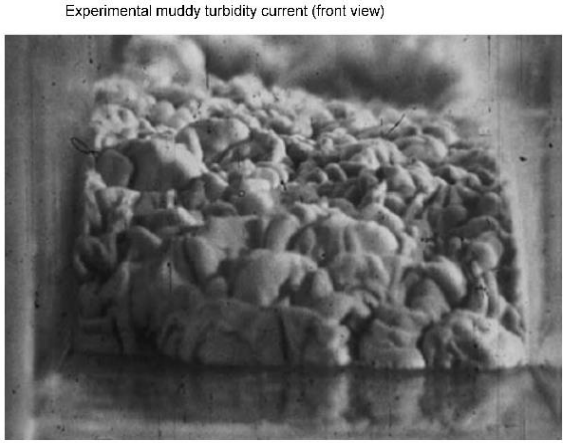

Fig. 14. Photograph of front view of experimental turbidity current showing flow turbulence. Photo from experiments conducted by M. L. Natland and courtesy of G. C. Brown. Published in Shanmugam, G. (2012). New perspectives on deep-water sandstones: origin, recognition, initiation, and reservoir quality. In: Handbook of petroleum exploration and production, vol. 9, 524 p. Amsterdam: Elsevier.

- Thin layers, commonly centimeters in thickness (core and outcrop) (Fig. 16)
- Sheet-like geometry in basinal settings (outcrop) (Fig. 17)
- Lenticular geometry may develop in channel-fill settings.

Fig. 15. Flute casts, common sole marks, often used as evidence for erosion by turbidity currents. Arrow = Flow direction from left to right. However, alternative interpretations by bottom currents are suggested (Klein, 1966). Jackfork Group, Pennsylvanian, Oklahoma. Photo by G. Shanmugam

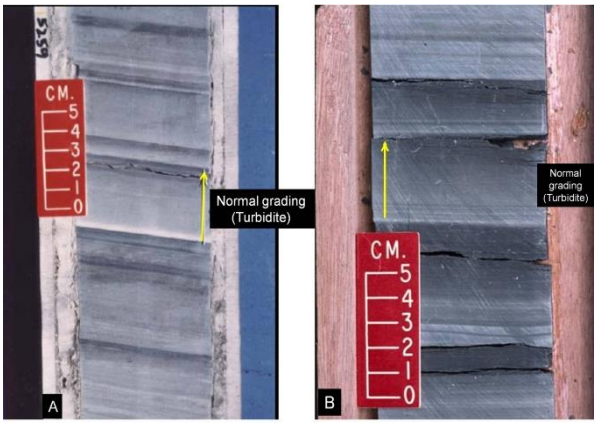

Fig. 16. Two examples of classic turbidites, (A) Core photograph showing turbidite units with sharp basal contact, normal grading, and gradational upper contact. Arrow marks a normally graded unit with fine-grained sand at bottom (light gray) grading into clay (dark gray) near top. Note that these thin-bedded units cannot be resolved on seismic data. Zafiro Field, Pliocene, Equatorial Guinea. From Shanmugam (2006). Elsevier, (B) Core photograph showing turbidite units with sharp basal contact, normal grading, and gradational upper contact (yellow arrow). Cretaceous, West Africa.

Problem

1) Misapplication of the term 'turbidite' for deposits of all four types of sediment-gravity flows, including debris flows (Fig. 18) by Mutti et al. (1999) and by Zavala (2019).
2) There is no agreement on the density value that separates "low-density" from "high-density" turbidity currents (Fig. 19A). Turbidity currents are inherently low in sediment concentration or low in flow density (Fig. 19A), According to Bagnold (1962), typical turbidity currents can function as truly turbulent suspensions only when their sediment concentration by volume is below 9% or c. < 9% (Fig. 19A). Therefore, high-density turbidity currents (Fig. 19B) cannot exist in nature.
3) Flume experiments have revealed that the so-called "high-density turbidity currents" are indeed composed of a basal laminar layer, typical of debris flows (Shanmugam, 1996), not turbulent turbidity currents. Experiment also provided evidence for deposition of floating clasts (Postma et al., 1988) at the rheological interface (Fig. 19B), which is common in debris flows.

Fig. 17. Outcrop photograph showing tilted thin-bedded turbidite sandstone beds with sheet-like geometry, Lower Eocene, Zumaya, northern Spain. Reproduced from Shanmugam (2006). Elsevier. Photo by G. Shanmugam.

4) The complete “Bouma sequence” (with Ta, Tb, Tc, Td, and Te divisions) has never been documented in modern deep-sea sediments. Nor has it been reproduced in flume experiments. Furthermore, this model suffers from a lack of sound theoretical basis (Leclair and Arnott, 2005; Sanders, 1965; Shanmugam, 1997). Leclair and Arnott (2005, p. 4) state that “. . .the debate on the upward change from massive (Ta) to parallel laminated (Tb) sand in a Bouma-type turbidite remains unresolved.” The ultimate objective of facies models is to interpret ancient strata (i.e., the unknown). However,

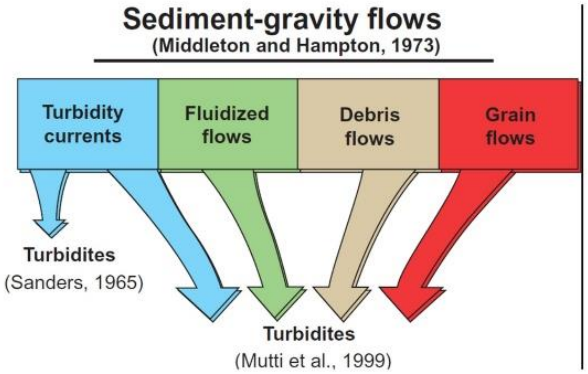

Fig. 18. Original classification of sediment-gravity flows by Middleton and Hampton (1973). Confusing application of the term 'turbidites' to deposits of all four types by Mutti et al. (1999) without regard for fluid mechanics, which Zavala (2019) has adopted in his comment. I have adopted Sanders' (1965) classification in which only deposits of turbidity currents are considered as turbidites. From Shanmugam (2002).

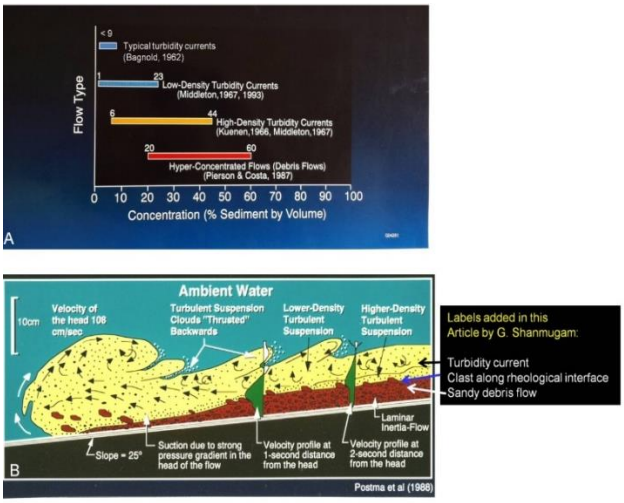

Fig. 19. (A)-Plot of sediment concentration for different flow types. Note that a typical turbidity current can exist only in sediment concentration less than 9% by volume (Bagnold, 1962). Note overlap in sediment concentration among low-density, turbidity currents, high-density turbidity currents, and hyper-concentrated flows. Modified after Shanmugam (1996). Reproduced with permission from SEPM. (B)-Experimental stratified flows with a basal laminar-inertia flow and an upper (turbulent) turbidity current that have been termed as “high-density turbidity currents.” Note clasts near the top of sandy debris flows along the rheological interface. Compare with Fig. 29 and related text. Figure from Postma et al. (1988). Publication: Sedimentary Geology. Elsevier

the turbidite facies models, developed exclusively from the ancient strata without validation from the modern environment (i.e., the known), promote circular reasoning

5) The ideal turbidite bed with 16 divisions (Fig. 20) is untenable from a fluid dynamic point of view. No one has ever documented the vertical facies model showing the R1, R2, R3, S1, S2, and S3 divisions of the Lowe (1982) sequence and the Ta, Tb, Tc, Td, and Te divisions of the Bouma (1962) sequence in ascending order in modern deep-sea sediments.
6) No one has ever replicated in flume experiments of turbulent turbidity currents that could carry coarse sand and gravel in suspension in laboratory flume experiments that could produce the R1, R2, R3, S1, S2, and S3 divisions in ascending order.

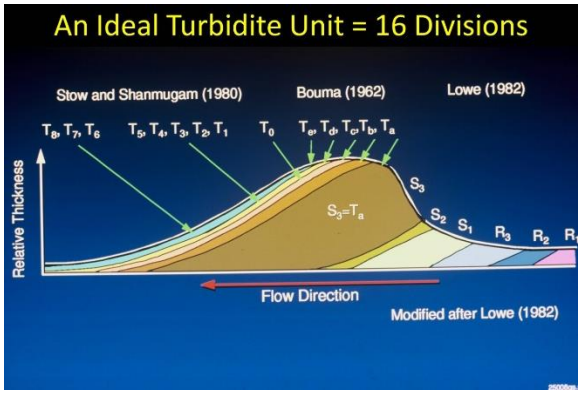

Fig. 20. An ideal turbidite bed should develop 16 divisions. However, no one has ever documented such a turbidite bed with 16 divisions in the field or in flume experiments. After Shanmugam (2000), reproduced with permission from Elsevier

Debris Flows

Definition

A debris flow is a sediment flow with plastic rheology and laminar state from which deposition occurs through freezing en masse. The terms debris flow and mass flow are used interchangeably because each exhibits plastic flow behavior with shear stress distributed throughout the mass (Nardin et al., 1979). In debris flows, inter-granular movements predominate over shear-surface movements. Although most debris flows move as incoherent mass, some plastic flows may be transitional in behavior between coherent mass movements and incoherent sediment flows (Marr et al., 2001). Debris flows may be mud-rich (i.e., muddy debris flows), sand-rich (i.e., sandy debris flows), or mixed types. In multibeam bathymetric data, recognition of debrites is possible.

Sandy debris flows are defined because of their importance in petroleum geology (Shanmugam et al., 2009). Sandy debris flow represents an intermediate stage between grain flow and cohesive debris flow (Fig. 2). The concept of sandy debris flows was first introduced by Hampton (1972). Sandy debris flows are defined here on the basis of (1) plastic rheology; (2) multiple sediment-support mechanisms (cohesive strength, frictional strength, hindered settling, and buoyancy); (3) mass-transport mode; (4) more than 25-30% sand and gravel; (5) 25-95% sediment (gravel, sand, and mud) concentration by volume (Fig. 5); and (6) variable clay content (as low as 0.5% by weight) (Shanmugam, 2000). Sandy debris flows could develop in slurries of any grain size (very fine sand to gravel), any sorting (poor to well), any clay content (low to high), and any modality (unimodal and bimodal). Sandy debris flow was misclassified as "high-density turbidity currents" (Shanmugam, 1996).

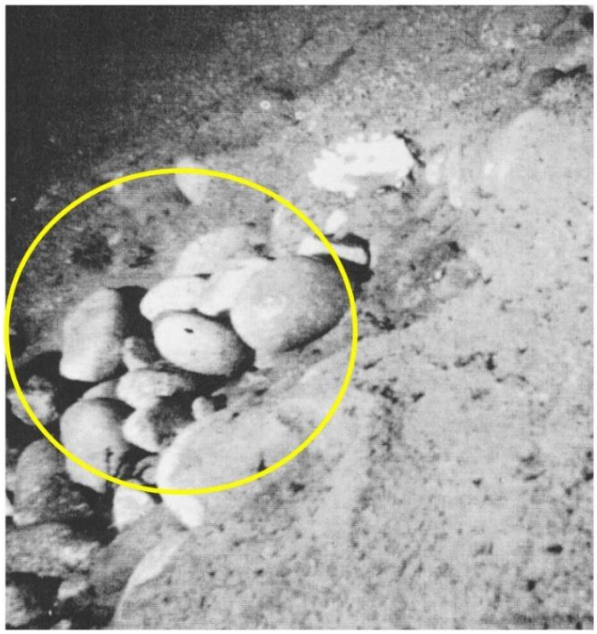

Fig. 21. Underwater photograph showing a pocket of rounded cobbles up to 15 cm in diameter in massive sandy matrix at a depth of 130 m (427 ft) in Los Frailes Canyon, Baja California. Note projected nature of clasts from the upper sediment surface. Photo by R.F. Dill. After Shepard and Dill (1966), Rand McNally & Company, Published in Shanmugam, G. (2012). New perspectives on deep-water sandstones: Origin, recognition, initiation, and reservoir quality. In: Handbook of petroleum exploration and production, vol. 9, 524 p. Amsterdam: Elsevier.

Origin

- Earthquake,
- slope instability on alluvial fans,
- oversupply of sediment,
- volcanism,
- meteorite impact,
- tsunamis, and
- cyclones.

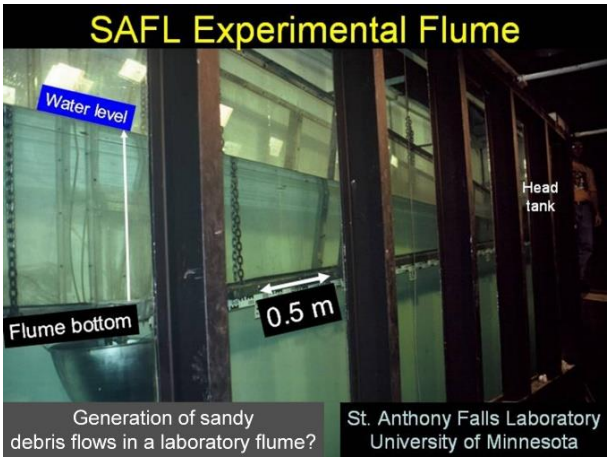

Fig. 22. Flume used in the experiments of sandy debris flows. See Shanmugam (2000) and Marr et al. (2001) for details on experiments. Photo by G. Shanmugam.

Identification

Debris flows are capable of transporting gravel and coarse-grained sand because of their inherent strength. General characteristics of muddy and sandy debrites are:

- Gravel to mud lithofacies.
- The reliability of identification of ancient debrites in the rock record is high. This is because reliable field criteria have been developed on the basis of modern analogs of gravelly debrites (Fig. 21) and on the basis of large laboratory flume (Fig. 22) experiments in reproducing excellent examples of sandy debris flows with various diagnostic features, such as snout (Fig. 23) and other identification markers (Fig. 23).
- Floating or rafted mudstone clasts near the tops of sandy or muddy beds (core and outcrop) (Fig. 25)
- Floating armored mudstone balls in sandy matrix (core and outcrop)
- Projected clasts (core and outcrop) (Fig. 25)
- Planar clast fabric (core and outcrop) (Fig. 26A)
- Imbricate clasts (experiment)
- Brecciated mudstone clasts in sandy matrix (core and outcrop) (Fig. 27)
- Concentration of larger clasts (pumice blocks) near the front of volcanic debris flows or lahars, which would result in inverse grading of clasts in the rock record
- Inverse grading of clasts and rock fragments with random fabric (core and outcrop) (Fig. 28)
- Inverse grading of quartz granules in sandy matrix (core and outcrop)
- Inverse grading, normal grading, inverse to normal grading, and absence of any grading of matrix (core and outcrop)
- Unusually large blobs of heterolithic facies in muddy matrix
- Floating quartz granules in sandy matrix (core and outcrop)
- Pockets of gravels in sandy matrix (core and outcrop) (Fig. 21)
- Preservation of delicate mud fragments with planar fabric in sandy matrix (core and outcrop)
- Irregular, sharp upper contacts (core and outcrop)
- Side-by-side occurrence of garnet granules (density: 3.5–4.3) and quartz granules (density: 2.65) (core and outcrop)
- Lenticular to sheet-like in geometry
- Lobe-like geometry (map view) in the Gulf of Mexico Tongue-like geometry (map view) in the North Atlantic (Fig. 27A).

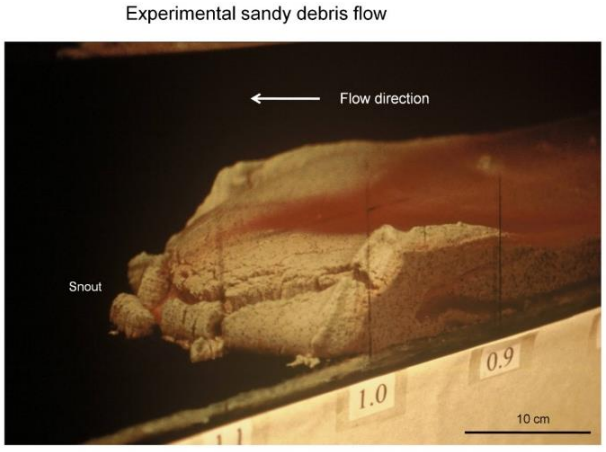

Fig. 23. Side view of flume tank showing strong debris flows with well-developed snout. Note the absence of turbulent suspension on top. Also note irregular upper surface caused by sudden freezing of the flow. Deformation in the front suggests strongly coherent character of flow, which may be called a slump. Reproduced from Shanmugam, G. (2006). Deep-water processes and facies models: Implications for sandstone petroleum reservoirs. In: Handbook of petroleum exploration and production, vol. 5, 476 p. Amsterdam: Elsevier

Features	Observation	Interpretation
	Sharp Upper Contact	Freezing of Flow and Plastic Rheology
	Irregular Upper Contact and Lateral Pinch-out Geometry	Freezing of Primary Relief and Plastic Rheology
	Irregular Front (Snout)	Freezing of Primary Relief and Plastic Rheology
	Non-Erosive Base and Water Entrapment (↙)	Laminar Flow and Hydroplaning
	Dish Structures and Water Entrapment (↙)	Hydroplaning and Water Escape
	Vertical Pipes	Hydroplaning and Water Escape
	Grain Segregation and Normal Grading	Grain Settling from Weak Flow
	Planar Fabric and Inverse Grading	Laminar Flow and Flow Strength
	Random Fabric	Flow Strength and Freezing of Flow
	Internal Layers	Mass Movement and Secondary Glide Planes
	Imbricate Slices	Mass Movement and Compression
	Isolated Blocks	Mass Movement and Tension
Flow Direction →	120 μm Silica Sand 500 μm Coal Slag (bulk density: 2.6 g/cm3)	

Fig. 24. Summary of identification markers associated with debris flows based on experiments. From Shanmugam (2000). Elsevier.

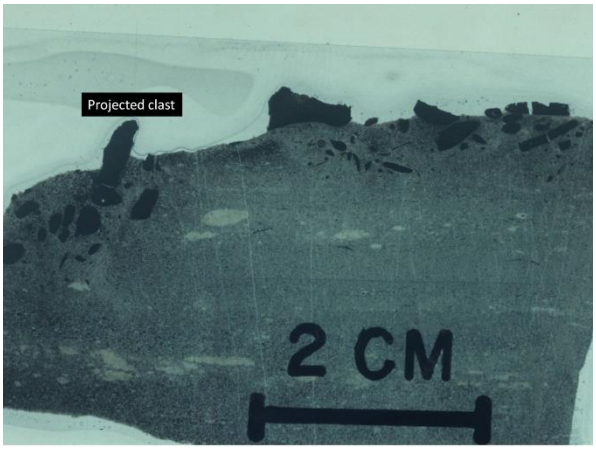

Fig. 25. Polished slab showing projected clasts, interpreted as freezing by debris flows. From Shanmugam and Benedict (1978). SEPM.

The modern Amazon submarine channel has two major debrite deposits (east and west) (Damuth and Embley, 1981; Piper et al., 1997). The western debrite unit is about 250 km long, 100 km wide and 125 m thick. In the U.S. Atlantic margin, debrite units are about 500 km long, 10-100 km wide, and 20 m thick. On the NW African Continental margin, the Canary debrite is 60-100 km wide, 5-20 m thick, and traveled about 600 km (Masson et al., 1997).

Based on (1) experimental sandy debris flows showing detached blocks (Shanmugam, 2000), (2) documented long runout natural sandy debris flows in modern oceans (Gee et al., 1999) and (3) interpreted example in the ancient record (Teale and Young, 1987), long runout sandy debrite blocks are viable candidates for developing thick, isolated, sandstone petroleum reservoirs in deep-water environments. Because of clay-poor nature (Marr et al., 2001), isolated outrunner sandy debrites have great potential for serving as sandstone petroleum reservoirs.

Problem

There are three major problem areas regarding interpreting coarse-grained deposits either as high-density turbidites or as sandy debrites in deep-water strata.

First, are high-density turbidity currents sandy debris flows? Conventionally, stratified flows have been classified as high-density turbidity currents. I (Shanmugam, 1996) argued against such classifications. The prevailing differences of opinion on nomenclature can be explained by our flume experiments (Shanmugam, 2000; Marr et al., 2001). For example, the stratified flow with lower laminar layer and an upper turbulent layer in our experiment (Fig. 29) would be classified differently by different researchers as follows:

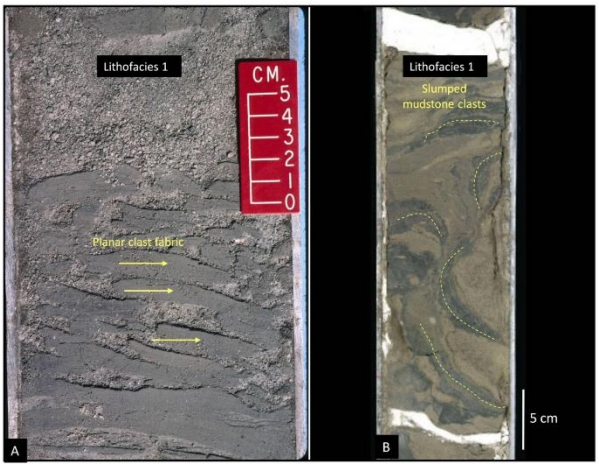

Fig. 26. Core photos showing planar clast fabric (A) and associated slump facies (B). Pliocene reservoir sands in upper-slope canyon environments, Offshore Krishna-Godavari Basin, Bay of Bengal (Iindia). From Shanmugam et al. (2009).

1. Group 1 of researchers would recognize the importance of bottom layer with different rheology and flow state (Bagnold, 1956; Sanders, 1965; 3; Shanmugam, 1996).
2. Group 2 would not (Kuenen, 1956; Postma et al., 1988; Mutti et al., 1999; Zavala, 2019). Postma et al. (1988) would combine both layers and classify them together as "High-density turbidity currents" (Fig. 19B).

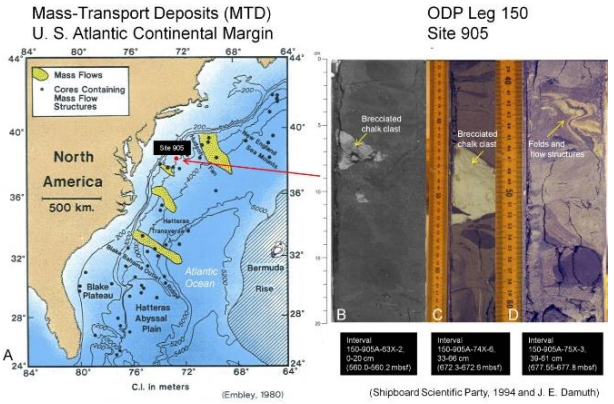

Fig. 27. (A) Map showing the distribution of MTD on the U.S. Atlantic Continental margin. Note position of ODP Leg 150, Site 905 (filled red circle) added in this study. (B) Core photograph showing brecciated chalk clast. (C) Core photograph showing brecciated chalk clast (Eocene) in sandy clay matrix. (D) Core photograph showing folds and flow structures in sandy clay matrix. Color photograph courtesy of J.E. Damuth. Red arrow points to site location. From Shanmugam (2017a). Elsevier.

Second, are floating clasts in deep-water sandstones representing sandy debrites? Experiments have shown that clasts indeed form along rheological boundaries on top of sandy debris flows (Fig. 19B).

Third, the major unresolved issue is flow transformation in sediment-gravity flows. Fisher (1983) proposed four types of transformations for sediment-gravity flows: (1) body transformation; (2) gravity transformation; (3) surface transformation; and (4) elutriation transformation. Flow transformations cannot be established without knowing: (1) initial flow behavior; (2) transport mechanisms; and (3) final flow behavior. There are, however, no established criteria for recognizing initial flow behavior and transport mechanisms in the depositional record (Dott, 1963; Middleton and Hampton, 1973).

In discussing the physics of debris flows, Iverson (1997) states, 'When mass movement occurs, the sediment-water mixtures transform to a flowing, liquid-like state, but eventually they transform back to nearly rigid deposits.' Although such transformations can occur during transport, evidence for flow transformations cannot be inferred from the final deposit. We may never resolve this issue of flow transformation.

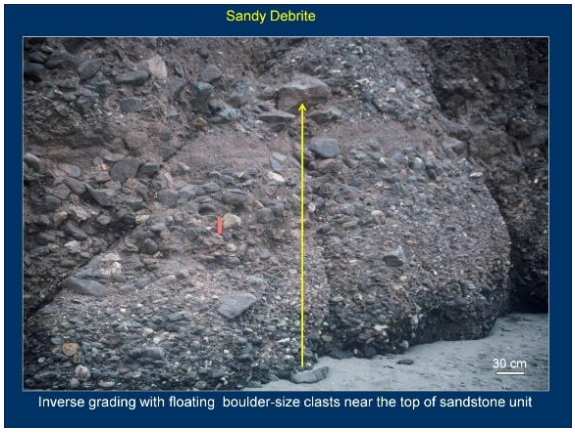

Fig. 28. Outcrop photograph showing inverse grading with floating boulder-size clasts near the top of sandstone unit (arrow). Note random fabric of clasts. Middle Miocene, San Onofre Breccia, Dana Point, California. This lithofacies has been interpreted to be sandy debrite associated with alluvial fan and fan delta. Reproduced from Shanmugam, G. (2012). New perspectives on deep-water sandstones: origin, recognition, initiation, and reservoir quality. In: Handbook of petroleum exploration and production, vol. 9, 524 p. Amsterdam: Elsevier

Liquefied/Fluidized Flows

Definition

In contrast to the classification of Middleton and Hampton (1973), Lowe (1976a) made a clear distinction between liquefied and fluidized systems. In liquefied beds and flows, the solids settle downward through the fluid, displacing it upward, whereas in fluidized beds, the fluid moves upward through the solids, which are temporarily suspended without netdo wnward movement.

Origin

- Earthquake,
- sediment loading,
- volcanism,
- meteorite impacts,
- tsunamis, and
- cyclones,

In understanding this type of phenomenon, one needs to discuss liquefaction. Allen (1984)

provided an accurate account of soft-sediment deformation in terms of physics.

1) Stratigraphical and sedimentological studies over many years have shown that soft sediments often become deformed non-tectonically. The structures induced take myriad forms and are increasingly called "soft-sediment deformations".

2) Soft-sediment deformation is associated in time with the earliest stages of sediment consolidation, when the deposit is weakest and pore fluid is being expelled most rapidly. This process is popularly known as "prelithification deformation". Lowe (1975) classified such soft-sediment deformations as "water-escape structures".

3) Liquefaction is significant in the production of many kinds of soft-sediment deformations.

He and Qiao (2015, their Fig. 1) classified deformations of seismites, based on structural styles, preserved positions, activity times, formation mechanisms and dynamics of soft-sediment deformation structures triggered by seismic activity, into 5 primary types:

(1) liquefied deformation,
(2) thixotropic deformation,
(3) hydroplastic deformation,
(4) superimposed gravity driving deformation, and,
(5) brittle deformation. Further, based on the main genetic types, composition of sediments and deformation styles, the authors proposed 35 secondary types (e.g., liquefied breccia, liquefied droplet, homogenite, tepee structure, fault grading, shatter breccia, etc.).

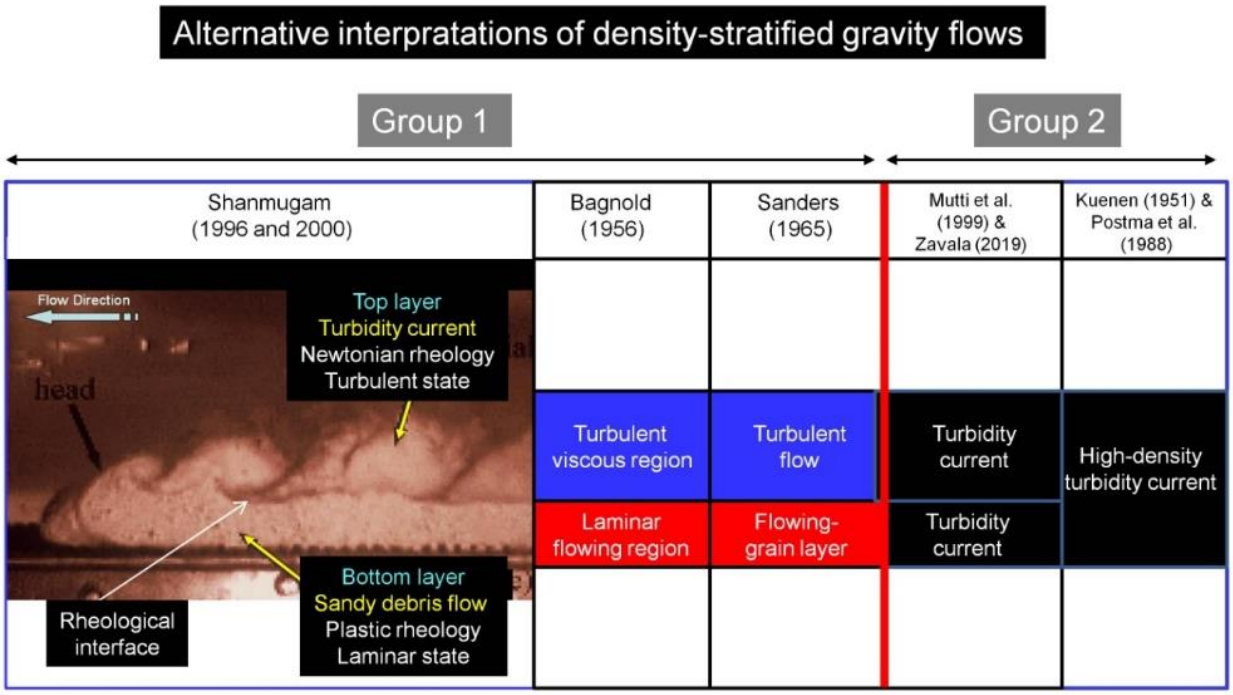

Fig. 29. Diagram illustrating the importance of distinguishing bottom layer based on fluid rheology and flow state in density-stratified gravity flows, which is based on a photograph of experimental density-stratified gravity flows showing the rheological difference between plastic debris flow (bottom layer) in massive sand and Newtonian turbidity current (top layer). Note that only Group 1 of researchers would recognize the importance of bottom layer with different rheology and flow state. Note that Postma et al. (1988) would classify both layers together as 'high-density turbidity current' (see Fig. 19B). This Mobil-funded experimental flume study was carried out at St. Anthony Falls Laboratory (SAFL), University of Minnesota (1996-1998) under the direction of Professor G. Parker to evaluate the fluid dynamical properties of sandy debris flows. Results were published in two major articles (Shanmugam, 2000; Marr et al., 2001).

Identification

- Fluid escape structures
- Dish and pillar structures (Fig. 30A)
- Dewatering pipes (Fig. 30B)
- Soft-sediment deformation structures (SSDS) (Fig. 31), (Shanmugam, 2017a).

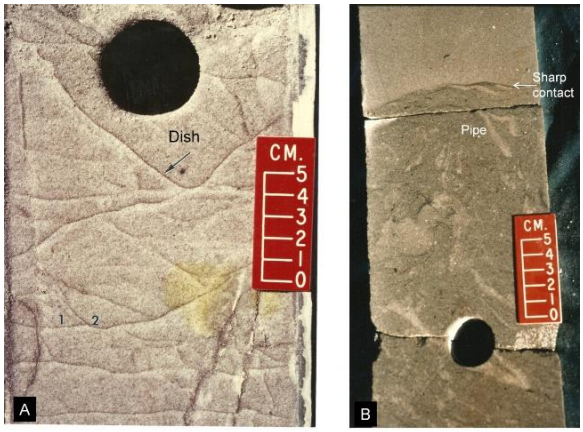

Fig. 30. (A)-Core photograph showing water-escape dish structures by liquidization in fine-grained, well-sorted sand. The arrow shows a concave-up (dish structure) color couplet with left wing dipping at 45º from the core horizontal due to deformation. Note cross-cutting relationship between two dish structures in which an earlier formed dish structure (1) has been terminated by a later one (2). Eocene, U.K. North Sea. From Shanmugam (2006), with permission from Elsevier; (B)-Core photograph showing pipes (water-escape structures). Paleocene, U.K. Atlantic Margin. Figures from Shanmugam (2012), with permission from Elsevier.

Su and Sun (2012) proposed that the following SSDS are common identification markers associated with earthquake-induced liquefaction:

- diapirs,
- clastic dikes,
- convolute bedding,
- compressional deformation features (accordion folds, plate-spine breccias, mound-and-sag structures), and
- extensional plastic features (loop-bedding).

Li et al. (2008) suggested the following criteria for recognizing features induced by seismicity:

- Seismic micro-fractures,
- microcorrugated laminations,
- liquefied veins, “vibrated liquefied layers”,
- deformed cross laminations,
- convolute laminations,
- load structures,
- flame structures, breccias,
- slump structures,
- seismo-disconformity.

Problem

Fluidized flows are transitional and transient in nature (Lowe, 1982). They also are not important sediment transport processes. For these reasons, I combined the two processes and call it 'Liquefied/Fluidized flow'. In the rock record, it is a challenge to distinguish liquefaction features induced by earthquakes from those generated by rapid sedimentation. The other problem is that there are no objective criteria to recognize earthquakes as a unique triggering mechanism (among 20 others) of soft-sediment deformation structures (SSDS) (Shanmugam, 2017b). Major problems in recognizing seismicity-induced SSDS are discussed by Shanmugam (2016a).

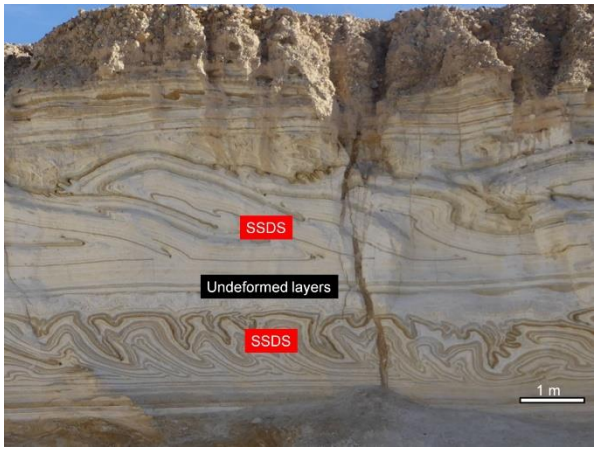

Fig. 31. Outcrop photograph showing two layers of seismicity-induced soft-sediment deformation structures (SSDS) with an intervening interval of undeformed layers. Perazim Wadi in the Quaternary Lisan Formation, a dry wash in the Ami'az Plain SW of Ein Boquet in Israel. Although this formation is not of deep-water origin, it illustrates the seismicity-induced sediment deformation in tectonically active settings. Photo courtesy of Professor Emeritus R. D. Hatcher, Jr., Department of Earth and Planetary Sciences, The University of Tennessee, Knoxville.

Grain Flows

Definition

According to Lowe (1976b), the term grain flow is restricted to sediment gravity flows in which a dispersion of cohesionless grains is maintained against gravity by grain dispersive pressure and in which the fluid interstitial to the grains is the same as the ambient

fluid above the flow. Modified flows include those in which a dense interstitial fluid, current, or escaping pure fluid aids in maintaining the dispersion.

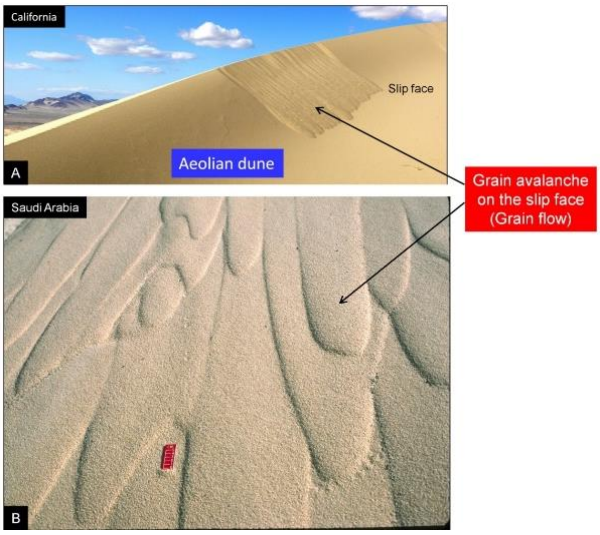

Fig. 32. Grain flows. (A). Photograph showing grain avalanches (i.e., grain flows) on the 'slip face' or lee side of an aeolian dune. Photo was taken at Kelso in the Mojave desert, California by Mark. A. Wilson. Wikipedia. Public domain. (B). Photograph showing grain avalanches (i.e., grain flows) on the 'slip face' or lee side of an aeolian dune. Saudi Arabia. Red scale = 5 cm.

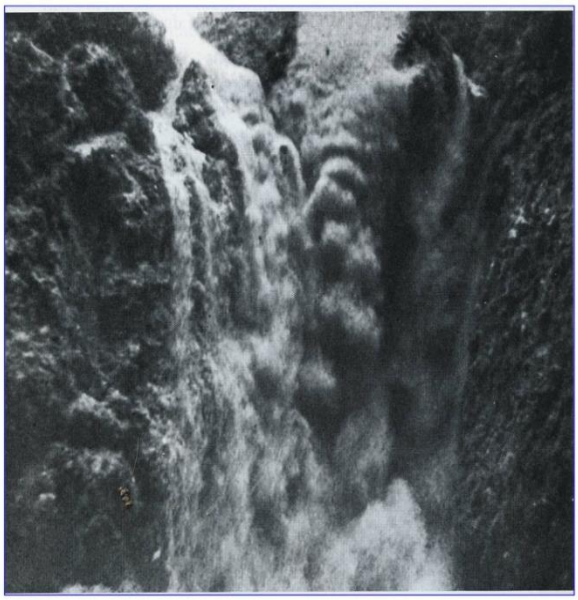

Fig. 33. Underwater photograph showing a cascading sand fall at a depth of 40 m (130 ft) in gully leading down into San Lucas Canyon, Baja California. Such pure sand falls would develop massive sand intervals in the rock record. Photo by R.F. Dill. After Shepard and Dill (1966), Rand McNally & Company.

Origin

- Arid climate, wind, aeolian dunes (Fig. 32)
- Steep gradients associated with submarine canyon-heads where sand fall occurs (Fig. 33). Submarine sand falls are considered somewhat analogous to grain flows.

Identification

- Massive sand layers
- Thin layers (< 5 cm)
- Well sorted
- Inverse grading

Problem

Deposits of grain flows are volumetrically insignificant in submarine environments, but included here for completeness.

Thermohaline- Contour currents

Definition

Thermohaline-induced bottom currents that follow regional bathymetric contours in deep-water (200 bathymetry) environments. They are called thermohaline contour currents (THCC) in this article.

Origin

Wust (1936) first documented the importance of deep-water masses in the Atlantic Ocean. Deep-water masses in the world's oceans are caused by differences in temperature and salinity. When sea ice forms in the polar regions due to freezing of shelf waters, seawater experiences a concurrent increase in salinity due to salt rejection and a decrease in temperature. The increase in the density of cold saline (i.e., thermohaline) water directly beneath the ice triggers the sinking of the water mass down the continental slope (Fig. 34) and the spreading of the water masses to other parts of the ocean (Fig. 35). These are called thermohaline water masses.

.**Antarctic Bottom Water (AABW)**

The origin of thermohaline water masses are best studied using the Antarctic Bottom Water (AABW) (Gordon, 2001, 2019; Gordon et al. 2013; Purkey et al. 2018, among others). The AABW is initiated as downslope gravity flows on the continental slope (Fig. 36). The AABW has a density of 0.03 g /cm^3 with temperatures ranging from −0.8 to 2 °C (35 °F), salinities from 34.6 to 34.7 psu. Being the densest water mass of the oceans (Purkey et al., 2018, AABW is found to occupy the depth range below 4000 m. The ABW (Antarctic bottom water) is formed

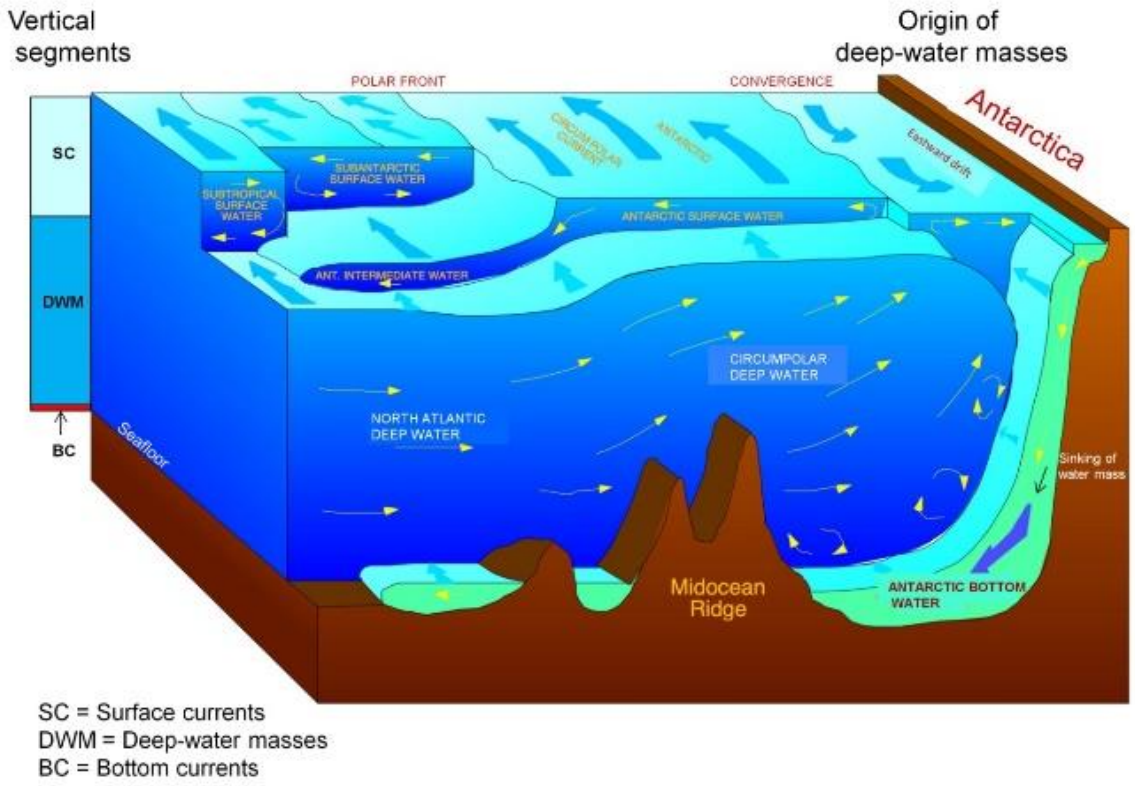

Fig. 34. A conceptual model of the Southern Ocean showing three vertical segments, composed of the upper surface currents, the middle deep-water masses, and the lower bottom currents, forming a vertical continuum (left). Note the origin of AABW by freezing of shelf waters (right). As a consequence, the increase in the density of cold saline (i.e., thermohaline) water triggers the sinking of the water mass down the continental slope and the spreading of the water masses to other parts of the ocean. Modified after Hannes Grobe, September 5, 2015. From Shanmugam (2012), with permission from Elsevier.

in the Weddell and Ross Seas, off the Adélie Coast and by Cape Darnley from surface water cooling in polynyas and below the ice shelf. A unique feature of Antarctic bottom water is the cold surface wind blowing off the Antarctic continent (Fig. 36). The surface wind creates the polynyas (i.e., an area of open water surrounded by sea ice), which opens up the water surface to more wind. This Antarctic wind is stronger during the winter months and thus the Antarctic bottom water formation is more pronounced during the Antarctic winter season. Stommel (1958) first developed the concept of the global circulation of thermohaline water masses and the vertical transformation of light surface waters into heavy deepwater masses in the oceans. Broecker (1991) presented a unifying concept of the global oceanic "conveyor belt" by linking the wind-driven surface circulation with the thermohaline-driven deep circulation regimes.

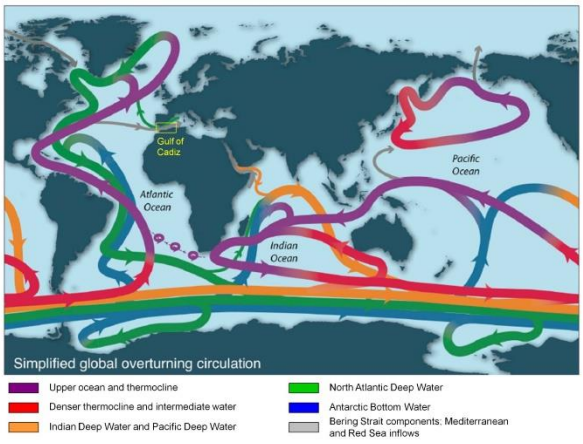

Fig. 35. Map showing the global overturning circulation (GOC). Note, the location of Gulf of Cadiz which served as the type locality for the contourite facies model. Modified after Talley (2013), with permission from the Oceanography Society.

The large-scale horizontal transport of water masses, which also sink and rise at select locations, is known as the "thermohaline circulation" or THC. Aspects of thermohaline circulation are discussed by Zenk (2008). The global overturning circulation has been presented by Talley (2013) (Fig. 35). Examples of selected deep-water masses in various parts of the world's oceans and their acronyms are given below.

AABW: Antarctic bottom water
ABW: Arctic bottom water
AAIW: Antarctic intermediate water (Brazilian margin)
ACC: Antarctic circumpolar current (Antarctica)
AW: Atlantic water (Mediterranean sea)
BC: Brazil current
BICC: Brazil intermediate counter current
CDW or CPDW: Circumpolar deep water
DGSRF: Deep Gulf Stream return flow
DWBUC or DWBC: Deep western boundary undercurrent
IDW: Indian deep water
ITF: Indonesian through flow
LCDW: Lower circumpolar deep water
LIW: Levantine intermediate water (Mediterranean sea)
MOW: Mediterranean outflow water
MUC: Mediterranean undercurrent
NADW: North Atlantic deep water
NAdDW: North Adriatic dense water
NPDW: North Pacific deep water (Japan)
NSDW: Norwegian sea deep water
PDW Pacific deep water
SACW: South Atlantic central water (Brazilian margin)
SOW: Sea overflow water
UCDW: Upper circumpolar deep water
WBUC: or WBU Western boundary undercurrent
WDW: Warm deep water (Antarctica)
WSBW: Weddell sea bottom water (Antarctica)
WSDW: Weddell sea deep water (Antarctica)

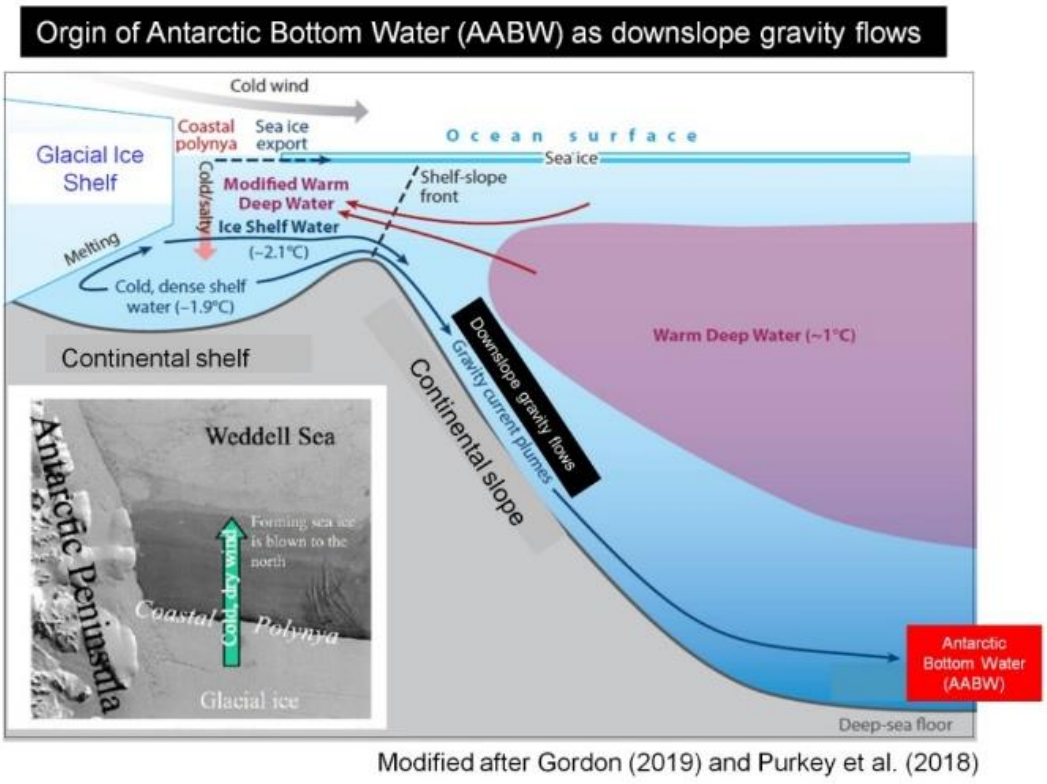

Fig. 36. Schematic of the origin of the Antarctic Bottom Water as downslope gravity flows on the continental slope. Cold shelf water forms through brine rejection in coastal polynyas during ice formation and export. The shelf water flows down the slope in dense plumes, mixing with ambient Warm Deep Water (also referred to as modified Circumpolar Deep Water). Potential temperatures pertinent to Weddell Sea Bottom Water formation are also shown. Modified after Gordon (2001, 2013) and Purkey et al. (2018) with additional labels by G. Shanmugam. Figure from Shanmugam (2020a).

The deep-water component of these water masses that winnow, rework, and deposit sediment on the seafloor for a sustained period of time is called 'thermohaline-induced bottom currents'. They often intersect with downslope turbidity currents or debris flows (Fig. 37) causing 'hybrid flows'. These thermohaline currents are known as 'contour currents' because of their tendency to follow bathymetric contours of continental slope and rise (Heezen et al., 1966). In addition to thermohaline-induced bottom currents or contour currents, there are three other major types, namely wind-driven, tide-driven, and internal tide-driven bottom currents (Shanmugam, 2016b). The genetic term 'contourite' was originally introduced for deposits of thermohaline-induced contour currents in the deep oceans (Hollister, 1967). Measured current velocities usually range from 1 to 20 cm/s (Hollister and Heezen, 1972); however, exceptionally strong, near-bottom currents with maximum velocities of up to 300 cm/s were recorded in the Strait of Gibraltar (Gonthier et al., 1984). Therefore, contour currents are quite capable of reworking sand and forming traction structures.

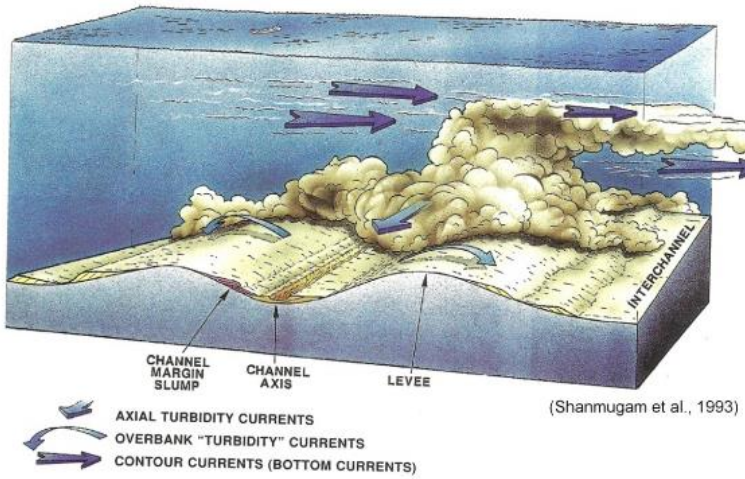

Fig. 37. Conceptual model showing the spatial relationship between downslope turbidity currents and along-slope contour currents. Intersection of these two flows are ideal for generating hybrid flows and their deposits (see Fig. 40), known as hybridites. After Shanmugam et al. (1993), AAPG

Identification

Traction structures (Fig. 38), such as ripple cross laminae and associated sharp upper contacts (Fig. 39), are common in contourites. The importance of traction structures in contourite has been documented worldwide (Hsü, 1964; Hubert, 1964; Klein 1966; Hollister 1967; Mutti, 1992; Shanmugam et al., 1993; Ito, 2002; Martın-Chivelet et al., 2008; Shanmugam, 2008)

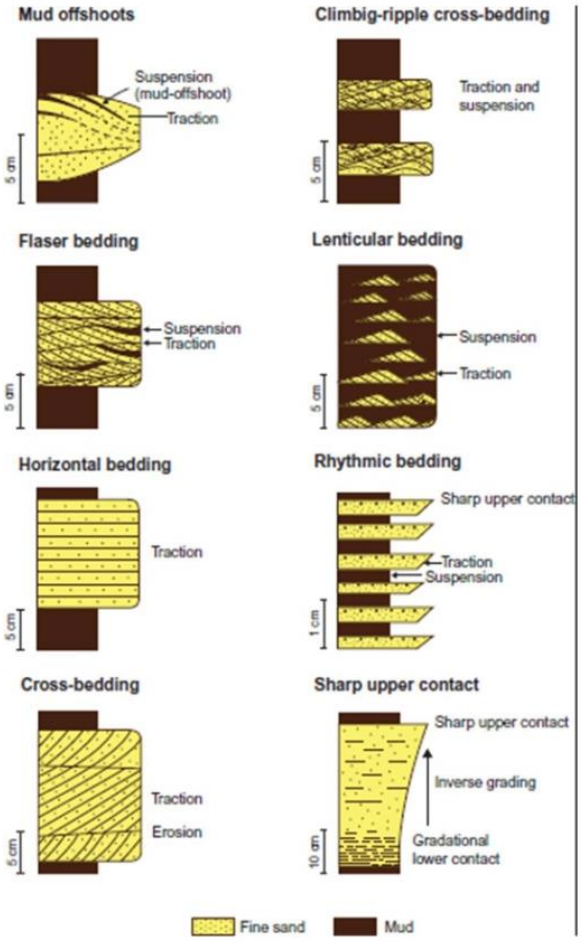

Fig. 38. Summary of traction features interpreted as indicative of deep-water bottom-current reworking by all types of bottom currents, namely thermohaline contour currents, wind-driven currents, tidal currents, and baroclinic currents (Shanmugam et al., 1993). Each feature occurs randomly and should not be considered as part of a vertical facies model. From Shanmugam et al., 1993, with permission from AAPG.

Problem

General problems associated with deep-water contourites are discussed by Shanmugam (2016b):
(1) In areas where both downslope sandy debris flows and alongslope bottom currents operate concurrently (Fig. 40A), the reworking of the tops of sandy debrites by bottom currents may be expected. Such a scenario, common on continental margins, could generate a basal massive sand division and an upper reworked division, mimicking a partial Bouma Sequence (Fig. 40B). Such offspring deposits of two flow types, namely sandy debris flows and contour currents (i.e., hybrid flows), are termed as "hybridites." These genuine hybrid flows should not be confused with the usage of the term "hybrid flows" by Houghton et al. (2009) for flow transformation from one gravity low into another. The distinction is that flow transformation represents a transitional stage between two flows, whereas, hybrid flows represent two hydrodynamically different flows without flow transition. The other difference is that hybrid flows travel at right angle to each other (i.e., downslope vs alongslope (Fig. 40A). Analogous to the

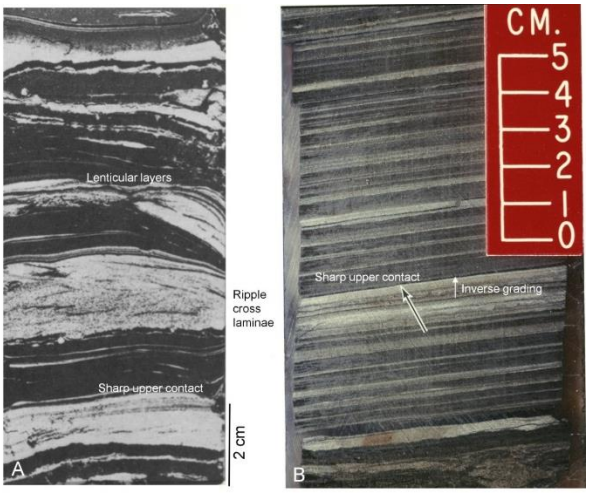

Fig. 39. (A) Core photograph showing well-sorted fine-grained sand and silt layers (light gray) with interbedded mud layers (dark gray). Note sand layers with sharp upper contacts, internal ripple cross-laminae, and mud offshoots. Also note lenticular nature of some sand layers. Pleistocene, continental rise off Georges Bank, Vema 18-374, 710 cm, water depth 4756 m. After Hollister (1967, his Figure VI-1, p. 208) and Bouma and Hollister (1973), reproduced with permission from SEPM. (B) Core photograph showing rhythmic layers of sand and mud, inverse grading, and sharp upper contacts of sand layers (arrow), interpreted as bottom-current reworked sands. Paleocene, North Sea. Figure from Shanmugam (2008).

concept of Houghton et al. (2009), Talling (2013) also proposed a transitional hybrid-flow model, using flow transformation, between turbidity currents and cohesive debris flows. Hybridites are common in the geologic record and could be easily misinterpreted as turbidites.

According to the Cambridge Dictionary, the term "hybrid" (Etymology: Latin word "Hybrida")

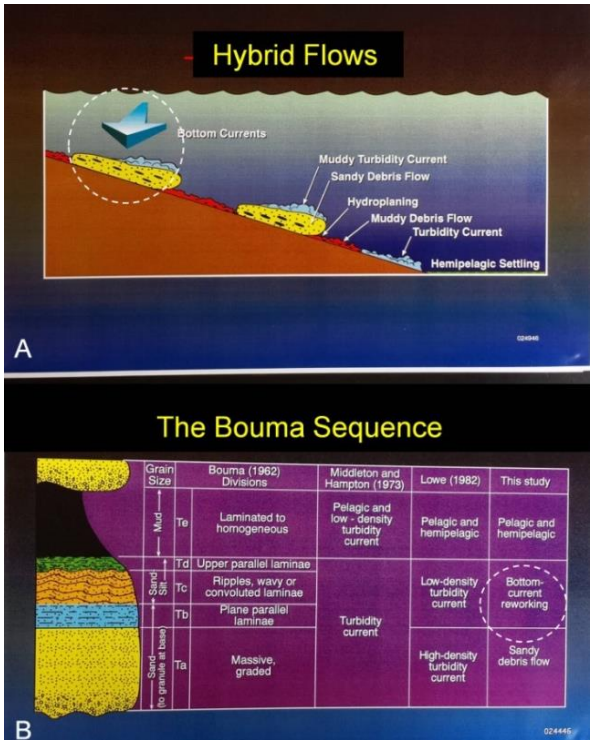

Fig. 40. (A) Conceptual model of genuine hybrid flows showing reworking (white circle) the tops of downslope sandy debris flows by alongslope bottom currents. (B) Such complex deposits would generate a sandy unit with a basal massive division and upper reworked divisions with traction structures (parallel or ripple laminae), mimicking the "Bouma sequence." (This may explain the upward transition of Ta to Tb, as discussed by Leclair and Arnott (2005). Source: (A) From Shanmugam (2006), with permission from Elsevier. (B) From Shanmugam (1997), with permission from Elsevier.

represents the hybrid offspring byproducts of two different plants, animals, or other entities (https://dictionary.cambridge.org/dictionary/learner-english/hybrid, accessed June 2, 2020). In animals, for example, a mule is the hybrid offspring of a male donkey and a female horse. By contrast, a debris flow often transforms downslope into a stratified flow with a lower debris-flow layer and an upper turbidity-current layer (Fig. 29) (see also Norem et al., 1990). In other words, the concept of "hybrid" begins with two different parental species yielding a single hybrid offspring whereas, the concept of "flow transformation"

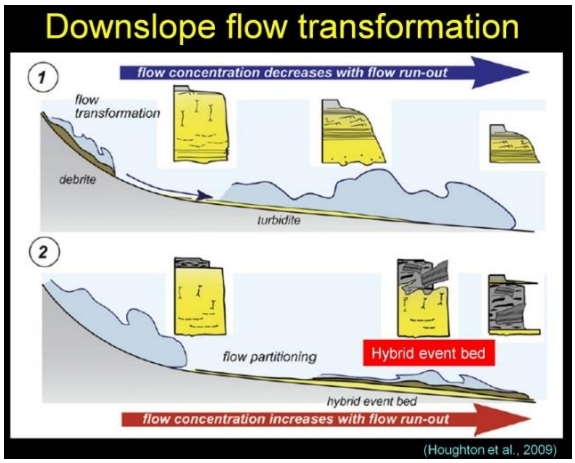

Fig. 41. Diagram showing "hybrid event beds" developed during flow transformation. Note that hybrid event beds do not follow the conventional etymological explanation of the term "hybrid" (see Fig. 42). From Houghton et al. (2009). Additional labels by G. Shanmugam.

begins with a single parent flow that transforms downslope into two sediment-gravity flows. Stratified flows are often called "high-density turbidity currents" (HDTC). Controversies surrounding HDTC were discussed by Shanmugam (1996). Flow transformations cannot be inferred from the final deposit. As noted earlier, we may never resolve this issue of flow transformation because it would be like attempting to establish the previous life history of a human being after reincarnation!

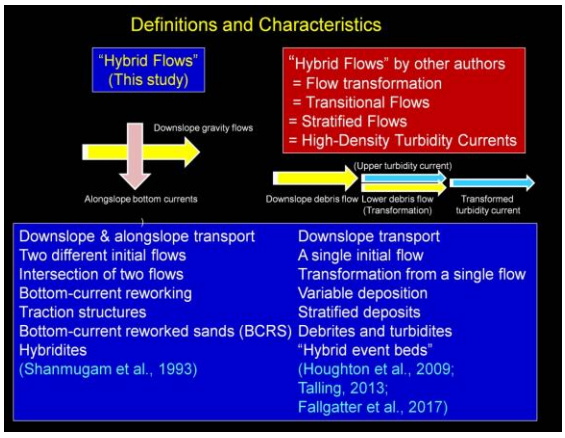

Fig. 42. Left: Genuine hybrid flows as used in this study by following etymology. Right: Equating hybrid flows with flow transformation as used by other authors by ignoring etymology

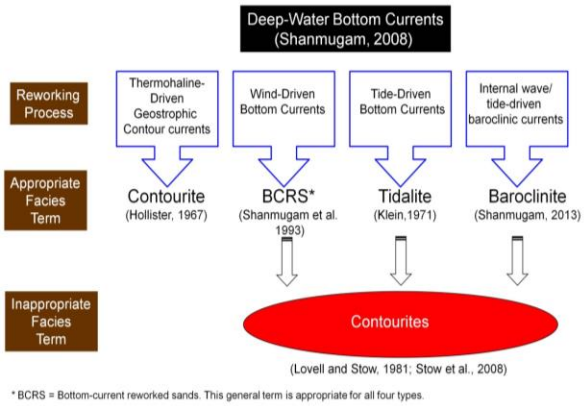

Fig. 43. Four types of bottom currents and their depositional facies. The facies term "contourites" is appropriate only for deposits of thermohaline-driven geostrophic contour currents, but not for deposits of other three types of bottom currents (i.e., wind, tide, or baroclinic). The basic problem began with a false narrative by Lovell and Stow (1981, p. 349) who state that ". . .the cause of the current is not necessarily critical to the application of the term." In other words, the term "contourites" can be applied to any kind of bottom-current deposit, irrespective of their origin (see also Stow et al., 2008).

(2) Traction structures are ubiquitous in bottom-current deposits of all kinds (Fig. 38). This has created problems in distinguishing deep-sea sediments with traction structures either as contourites (Bouma and Hollister, 1973) or as deposits of wind-driven bottom currents or as deposits of tidal bottom currents (see Shanmugam, 2008).

(3) In contrast to the original definition of contourites by Hollister (1967), Lovell and Stow (1981, p. 349) concluded that contourites can be produced by any kind of bottom current (Fig. 43), irrespective of their origin (i.e., thermohaline, wind, tide, or baroclinic). In maintaining clarity, it is suggested in this article to follow the original definition of contourites by Hollister (1967), which is to restrict the term "contourites" exclusively to the deposits of thermohaline-induced geostrophic contour currents in deep-water environments.

(4) The Gulf of Cadiz (Fig. 35), which served as the type locality for the contourite facie model (Fig. 44), is a highly complicated oceanographic location for studying depositional and erosional aspects of genuine contour currents. Furthermore, the vertical facies model suffers for the following reasons. First, the conventional explanation of the vertical change in grain size of the contourite facies model by changes in current velocity (Fig. 44) fails to consider alternative possibilities, such as increased sediment supply (Mulder et al., 2013)."

Second, the hydrodynamic origin of the five internal divisions is not understood in the Gulf of Cadiz. Third, the presence of internal hiatuses (Fig. 44) argues against the model being the product of a single depositional event. Fourth, bioturbation, considered to be a characteristic feature of contourites, is also common in turbidites and hyperpycnites (Shanmugam, 2018c). Fifth, the currents that operate in the Gulf of Cadiz are not genuine contour currents (Zenk, 2008), they represent a complex transitional type due to mixing and spreading (Shanmugam, 2016b, his Fig. 9.18). The five internal divisions (C1, C2, C3, C4, C5) in the model are not evident in the published core details from the IODP (Integrated Ocean Drilling Program) Expedition 339 (Shanmugam, 2016b).

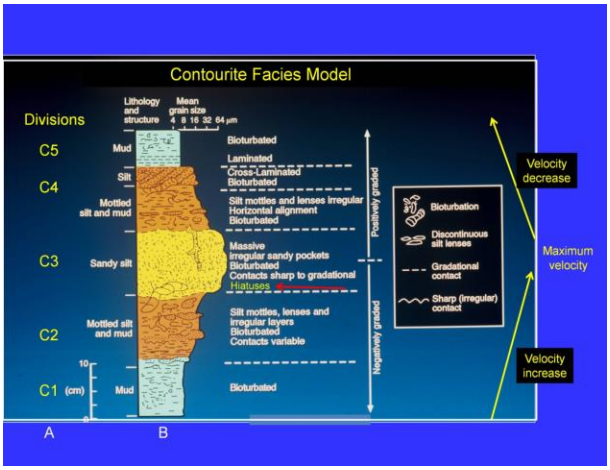

Fig. 44. (A). Revised contourite facies model with five divisions proposed by Stow and Faugères (2008). (B). Original contourite facies model by Gonthier et al. (1984). Note that the original authors of this model did not include the five internal divisions (Gonthier et al., 1984). The most recent version of this model by Faugères and Mulder (2011) contains neither the five internal divisions nor the hiatuses in the C3 division (red arrow inserted in this article). Note the similarity in vertical grain-size trend (inverse to normal grading) between hyperpycnite model (Fig. 8) and contourite model. Note that the ascending five divisions C1 to C5 in Fig. 44A were inadvertently listed in descending order in Shanmugam (2020a, his Fig. 8.17). Also note that the original muddy contourite facies model was published in the same year 1984 by both Gonthier et al. (1984) and by Faugères et al. (1984), Figure 44 B from Faugères et al. (1984), with permission from the Geological Society of America.

(5) Surprisingly, no one could explain the striking similarity in vertical grain-size trend (inverse to normal grading) between hyperpycnite model (Fig. 8) and contourite model (Fig. 44). Although Mulder et al. (2003) originally proposed the hyperpycnite facies model with inverse to normal grading (Fig. 8), Mulder et al. (2011) critiqued the contourite facies model with identical inverse to normal grading (Fig. 44).

(6) Gonthier et al. (1984, their Fig. 12) originally published the model *without* five internal divisions of C1-C5 and *without* hiatus at the bottom of the sandy interval (C5) in the middle (Fig. 44B). Stow and Faugères (2008, their Fig. 13. 9) published the model *with* five internal divisions of C1-C5 and *with* hiatus at the bottom of the sandy interval (C5) in the middle (Fig. 44A). One wonders as to why it took 24 years for Stow and Faugères (2008) to recognize five internal divisions and hiatus, if these features have been an integral part of contourite facies since its emplacement?

(7) Stow and Smillie (2020) proposed large-scale cross bedding in medium- to coarse sands for "The sandy contourite family" based on the study of Brackenridge et al. (2018). However, Brackenridge et al. (2018) did not document large-scale cross bedding in contourite sands. Stow and Smillie (2020) may prove to be correct because the likelihood of developing large-scale cross bedding by bottom currents is much greater than by turbidity currents.

(8) Stow and Smillie (2020, their Fig. 13) proposed base-cut-out contourites and top-cut-out contourites. Walker (1965) originally applied this "cut-out" logic to the Bouma Sequence. This approach assumes that the entire sequence was present at the time of deposition, but portions were cut-out. If this were true, one could assume anything to arrive at a desired interpretation, such as turbidite, contourite, tidalite, or seismite! Process interpretations must be based on observations and not on assumptions. In practice, it is difficult to verify one's assumptions without objective criteria.

(9) de Castro et al. (2020) reported bottom- current reworked sands (BCRS) in the Gulf of Cadiz (their Fig. 13). Although they reported starved ripples in the sandy intervals, but were unable to document with the empirical photographic evidence due to poor preservation of primary sedimentary structures in unconsolidated sediment intervals. It is important, however, to note that these authors were able to document wispy and lenticular laminae in their Facies 4 of sandy intervals (their Fig. 4), indicating bottom-current reworking in a sand-starved system.

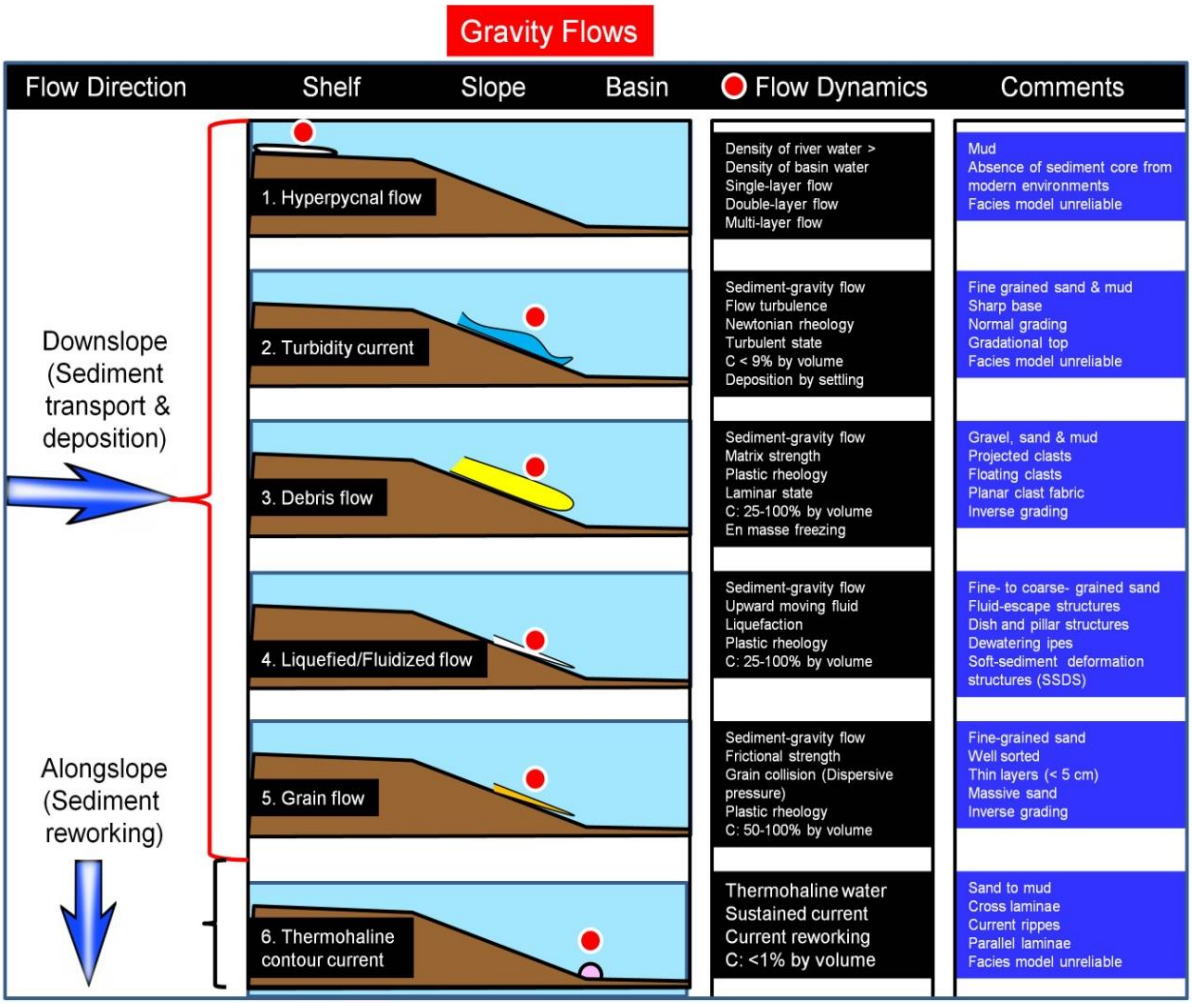

Fig. 45. Summary diagram of six types of gravity flows and their characteristics. Red dot denotes position of flow. From Shanmugam (2020a).

Concluding remarks

Gravity flows constitute the single most important sediment-transport mechanism on land, shelf, slope, and basin environments. They play important roles not only in downslope, but also in alongslope directions (Fig. 45). In terms of transporting large volumes of coarse-grained sediment in the deep sea, debris flows and related mass movements are the most important of all other processes. Also, identification markers of debrites discussed in this review are of value for recognizing them in the ancient sedimentary record because sandy debrites are important petroleum reservoirs worldwide. Of the six density flow types discussed, hyperpycnal flow is the least understood.

Acknowledgements

I thank Prof. G. M. Bhat, Managing Editor of JIAS, for encouraging me to submit this review. I also thank Prof. F.J. Hernández-Molina and Dr. S. de Castro, both of Royal Holloway, University of London, UK, who helped me with research material from IODP Expedition 339, Gulf of Cadiz. I wish to thank Professor Emeritus R. D. Hatcher, Jr., Department of Earth and Planetary Sciences, The University of Tennessee, Knoxville, TN. for providing a photo of SSDS from Israel Photo of Elwha River plume was courtesy of Tom Roorda, Roorda Aerial, Port Angeles, WA. A Mobil-funded experimental flume study was carried out at St. Anthony Falls Laboratory (SAFL), University of Minnesota (1996–1998) under the direction of Professor G. Parker to evaluate the fluid dynamical properties of sandy debris flows. Results were published in two major articles (Shanmugam 2000; Marr et al. 2001). I am grateful to the Reliance Industries Ltd. (RIL) in Mumbai (India) for the opportunity to examine cores from the offshore Krishna-Godavari Basin, Bay of

Bengal (Fig. 26)). As always, I am thankful to my wife Jean Shanmugam for her general comments.

References

Allen, J.R.L. (1970). Physical Processes of Sedimentation. Elsevier, New York, p. 239.

Allen, J.R.L., 1984. Sedimentary Structures, their Character and Physical Basis. Elsevier, Amsterdam, I, p. 593 and II, p. 663.

Allen, J.R.L. (1985a). Loose-boundary hydraulics and fluid mechanics, selected advances since 1961. In: Brenchley, P.J., Williams, P.J. (Eds.), Sedimentology, Recent Developments and Applied Aspects, Published for the Geological Society. Blackwell Scientific Publications, Oxford, pp. 7-28.

Allen, J.R.L. (1985b). Principles of Physical Sedimentology. George Allen & Unwin, London, p. 272.

Bagnold, R. A. (1954). Experiments on a gravity-free dispersion of large solid spheres in a Newtonian fluid under shear. Proc. R. Soc. Lond. A 225, 49–63.

Bagnold, R.A. (1956). The flow of cohesionless grains in fluids. Phil. Trans. Royal Society of London, Series A. Mathematical and Physical Sciences, 249, 235–297.

Bagnold, R.A. (1962). Auto-suspension of transported sediment. Philosophical Transactions of the Royal Society of London. Series A, Mathematical and Physical Sciences, 265, 315-319.

Bates, C.C. (1953). Rational theory of delta formation. AAPG Bulletin, 37 (9), 2119–2162

Bouma, A.H. (1962). Sedimentology of Some Flysch Deposits: A graphic approach to facies interpretation. Elsevier, Amsterdam, p. 168.

Beicher, R. J. (2000). Physics for Scientists and Engineers. Orlando: Saunders College.

Bouma, A.H., Hollister, C.D. (1973). Deep ocean basin sedimentation. In: Emiddleton, G.V., Bouma, A.H. (Eds.), Turbidites and Deep-Water Sedimentation. SEPM, Anaheim, CA, SEPM Pacific Section Short Course, pp. 79-118.

Breien, H., De Blasio, F. V., Elverhøi, A., Nystuen, J. P., and Harbitz, C. B. (2010). Transport mechanisms of sand in deep-marine environments—insights based on laboratory experiments: Journal of Sedimentary Research, 80, 975–990.

Broecker. W.S. (1991). The great ocean conveyor. Oceanography, 4, 79–89.

Coussot, P., Meunier, M. (1996). Recognition, classification and mechanical description of debris flows. Earth-Sci. Rev. 40, 209-227.

Dott Jr., R.H. (1963). Mechanics of subaqueous gravity depositional processes. AAPG Bulletin, 47, 104-128.

Damuth, J.E. Embley, R.W. (1981). Mass-transport processes on Amazon Cone: Western Equatorial Atlantic. American Association of Petroleum Geologists Bulletin, 65, 629–643.

Duda, J.J., Warrick, J.A., Magirl, C.S. (2011). Coastal and Lower Elwha River, Washington, Prior to Dam Removal—History, Status, and Defining Characteristics. In: Duda, J.J., Warrick, J.A., Magirl, C.S., (Eds.), Coastal Habitats of the Elwha River: Biological and Physical Patterns and Processes Prior to Dam Removal. U.S. Geological Survey Scientific Investigations Report 2011-5120. Chapter 1.

Embley, R.W. (1980). The role of mass transport in the distribution and character of deep-ocean sediments with special reference to the north Atlantic. Marine Geology, 38, 23–50.

Enos, P. (1977). Flow regimes in debris flow. Sedimentology, 24, 133_142.

Faugères, J.-C., Mulder, T. (2011). Contour currents and contourite drifts. In: Hüneke, H., Mulder, T. (eds.), Deep-Sea Sediments, Developments in Sedimentology 63: Elsevier, Amsterdam, pp. 149-214. Chapter 3.

Faugères, J.-C., Gonthier, E., Stow, D. A. V. (1984). Contourite drift moulded by deep Mediterranean outflow. Geology, 12, 296–300.

Feng, Z-Z. (2019). "Words of the Editor-in-Chief — Some ideas about the comments and discussions of hyperpycnal flows and hyperpycnites". *Journal of Palaeogeography*, 8

Fisher, R.V., (1983). Flow transformations in sediment gravity flows. Geology, 11, 273-274.

Forel, F.A. 1885. Les ravins sous-lacustres des fleuves glaciaires. Comptes Rendus de l'Académie des Sciences Paris, 101 (16), 725–728.

Forel, F.A. 1892. Le Léman: monographie limnologique. Vol. 1, 543. Lausanne: F. Rouge.

Galay, V. (1987). Erosion and Sedimentation in the Nepal Himalaya. Kefford Press, Singapore, p. 10, 11.

Gao, S., D. Wang, Y. Yang, L. Zhou, Y. Zhao, W. Gao, Z. Han, Q. Yu, and G. Li. (2015). Holocene sedimentary systems on a broad continental shelf with abundant river input: Process–product relationships. In River-dominated shelf sediments of east Asian seas, ed. P.D. Clift, J. Harff, J. Wu, and Y. Qui, vol. 429, 223–259. London: Geological Society, Spl Publ..

Gee, M.J.R., Masson, D.G., Watts, A.B., Allen, P.A. (1999). The Saharan debris flow: an nsight into the mechanics of long-runout submarine debris flows. Sedimentology 46, 317-335.

Gordon, A.L. (2001). Bottom water formation. In *Encyclopedia of Ocean Sciences*, 2nd edition, 334-340. Elsevier

Gordon, A.L. (2013). Bottom water formation. In *Encyclopedia of Ocean Sciences*, ed. JH Steele, KK Turekian, SA Thorpe, pp. 415–21. San Diego, CA: Academic. 2nd ed. https://doi.org/10.1016/B978-0-12-409548- 9.04019-7

Gordon, A.L. (2019). Bottom water formation. *Encyclopedia of Ocean Sciences*, Third Edition, 6, 120-126.

Hampton, M. A. (1972). The role of subaqueous debris flows in generating turbidity currents. Journal of Sedimentary Petrology, 42, 775-793.

He, B.Z., Qiao, X.F. (2015). Advances and overview of the study on paleo-earthquake events: a review of seismites. Acta Geologica Sinica (English Edition), 89, 1702-1746.

Heezen, B.C., Ewing, M. (1952). Turbidity currents and submarine slumps, and the 1929 grand banks earthquake. American Journal of Science, 250, 849-873.

Heezen, B.C., Hollister, C.D., Ruddiman, W.F. (1966). Shaping of the continental rise by deep geostrophic contour currents. Science, 152, 502-508. Henze, C. (2015). Antarctic Bottom Water in CMIP5 models: characteristics, formation, evolution. University of East Anglia, School o Environmental Sciences, Ph.D. Thesis. Norwich, England, UK. 226 p.

Hollister, C. D. (1967). *Sediment distribution and deep circulation in the western North Atlantic*, p. 467. Ph.D. dissertation, Columbia University, New York.

Houghton, P., Davis, C., McCaffrey, W. & Barker, S. (2009). Hybrid sediment gravity flow deposits – Classification, origin

and significance. Marine and Petroleum Geology, 26, 1900–1918.

Hsü, K. J. (1964). Cross-laminated sequence in graded bed sequence. *Journal of Sedimentary Petrol.ogy*, 34, 379–388.

Hubert, J.F. (1964).Textural evidence for deposition of many western North Atlantic deep-sea sands by ocean-bottom currents rather than turbidity currents. *The Journal of Geology*, 72, 757-785

Ito, M. (2002). Kuroshio current-influenced sandy contourites from the Plio-Pleistocene Kazusa forearcbasin, Boso Peninsula, Japan. In: D.A.V. Stow , C.J. Pudsey , J.A. Howe , J.-C. Faugères , A.R. Viana (eds.). Deep-Water Contourite Systems: Modern Drifts and Ancient Series, Seismic and Sedimentary Characteristics Geological Society Memoir vol. 22, pp. 421-432

Iverson, R. M. (1997). The physics of debris flows. Reviews of Geophysics, 35, 245-296.

Klein, G.D. (1966). Dispersal and petrology of sandstones of Stanley-Jackfork boundary, Ouachita foldbelt, Arkansas and Oklahoma. AAPG Bulletin, 50, 308-326.

Klein, G.D. (1971). A sedimentary model for determining paleotidal range. Geological Society of America Bulletin, 82, 2585–2592.

Klein, G.D. (1975). Resedimented pelagic carbonate and volcaniclastic sediments and sedimentary structures in Leg 30 DSDP cores fromthewestern equatorial Pacific. Geology, 3, 39-42.

Kneller, B. (1995). Beyond the turbidite paradigm: physical models for deposition of turbidites and their implications for reservoir prediction. In: Hartley, A.J., Prosser, D.J. (Eds.), Characterization of Deep-Marine Clastic Systems, Geological Society Special Publication No. 94, pp. 31–49.

Kuenen, Ph. H. (1951). Properties of turbidity currents of high density. In: Hough, J.L. (Ed.), Turbidity currents and the transportation of coarse sediments to deep water. A Symposium, SEPM Special Publication 2, pp. 14–33.

Kuenen, Ph. H. (1953). Significant features of graded bedding. AAPG Bulletin, 37: 1044–1066.

Kuenen, Ph.H. (1966). Experimental turbidite lamination in a circular flume. J.Geol. 74, 523-545. Leclair, S. Arnott, R.W.C (2005). Parallel lamination formed by high-density turbidity currents. Journal of Sedimentary Research, 75, 1–5.

Li, S., Du, Y., Zhang, Z., Wu, J. (2008). Earthquake-related soft sediment deformation structures in Palaeogene on the continental shelf of the East China Sea. Frontiers of Earth Science, 2(2) : 177-186. http://dx.doi.org/10.1007/s11707-008-0026-9 (in Chinese with English abstract).

Lovell, J.P.B. and Stow, D.A.V. (1981). Identification of ancient sandy contourites. Geology, 9, 347–349.

Lowe, D.R. (1975). Water escape structures in coarse grained sediments. Sedimentology, 22, 157-204.

Lowe, D.R. (1976a). Subaqueous liquefied and fluidized sediment flows and their deposits. Sedimentology, 23, 285–308.

Lowe, D.R. (1976b). Grain flow and grain flow deposits. Journal of Sedimentary Petrology, 46, 188-199.

Lowe, D.R. (1979). Sediment gravity flows: their classification, and some problems of application to natural flows and deposits. In: Doyle, L.J., Pilkey, O.H. (Eds.), Geology of Continental Slopes, SEPM Special Publication 27, pp. 75–82.

Lowe, D.R. (1982). Sediment gravity flows: II. depositional models with special reference to the deposits of high-density turbidity currents. Journal of Sedimentary Petrology, 52, 279–297.

Marr, J.G., Harff, P.A., Shanmugam, G., Parker, G. (2001). Experiments on subaqueous sandy gravity flows: the role of clay and water content in flow dynamics and depositional structures. GSA Bulletin, 113, 1377–1386

Masson, D.G., van Niel. B., and Weaver. P.P.E. (1997). Flow processes and sediment deformation in the canary debris flow on the NW African continental rise. Sedimentary Geology, 110, 163–179.

Meckel, T. (2010). Classifying and characterizing sand-prone submarine mass-transport deposits, AAPG Annual Convention and Exhibition, New Orleans, LA, 11–14 April 2010 (Search and Discovery Article #50270 (Posted 16 July 2010)http://www.searchanddiscovery.com/documents/2010/50270meckel/ndx_meckel.pdf (Accessed June 19, 2019).

Meckel, L.D. III, Shipp, et al. (2011). Reservoir characteristics and classification of sand-prone submarine mass-transport deposits. In: Mass-transport deposits in deepwater settings, pp. 423–454. Tulsa, OK: SEPM. Special Publication No. 96.

Middleton, G.V. (Ed.), (1965). Primary Sedimentary Structures and their Hydrodynamic Interpretation. SEPM Special Publication 12, p. 265.

Middleton, G.V. (1966). Experiments on density and turbidity currents. I. Motion of the head. Canadian Journal of the Earth Science, 3, 523–546.

Middleton, G.V. (1967). Experiments on density and turbidity currents: III. deposition of sediment. Canadian Journal of Earth Sciences, 4, 475–505.

Middleton, G.V. (1970). Experimental studies related to problems of flysch sedimentation. In: Lajoie, J. (Ed.), Flysch Sedimentology in North America, Geological Association of Canada Special Paper No. 7, pp. 253–272.

Middleton, G.V. (1993). Sediment deposition from turbidity currents. Annual Review Earth Planetary Sciences, 21, 89–114.

Middleton, G.V., Bouma, A.H. (Eds.), (1973). Turbidites and Deep-water Sedimentation. SEPM Pacific section Short Course, Anaheim, California, p. 157.

Middleton, G.V., Hampton, M.A. (1973). Sediment gravity flows: mechanics of flow and deposition. In: Middleton, G.V., Bouma, A.H. (Eds.), Turbidites and Deep-water Sedimentation, SEPM Pacific section Short Course, Anaheim, California, pp. 1–38.

Middleton, G.V., Wilcock, P.R. (1994). Mechanics in the Earth and Environmental Sciences. Cambridge University Press, Cambridge, p. 459.

Morales de Luna, T., E.D. Fernández Nieto, and M.J. Castro Díaz. (2017). Derivation of a multilayer approach to model suspended sediment transport: Application to hyperpycnal and hypopycnal plumes. Communications in Computational Physics, 22 (5), 1439–1485.

Mulder, T., J.P.M. Syvitski, S. Migeon, J.-C. Faugères, and B. Savoye. (2003). Marine hyperpycnal flows: Initiation, behavior and related deposits. A review. Marine and Petroleum Geology, 20, 861–882.

Mulder, T., Hassan, R., Ducassou, E., Zaragosi, S., Gonthier, E., Hanquiez, V., Marchès, E., and Toucanne, S. (2013). Contourites in the Gulf of Cadiz: A cautionary note on

potentially ambiguous indicators of bottom current velocity. Geo-Marine Letter, 33, 357–367.

Mullins, H.T, Neumann A.C, Wilber RJ, Hine A.C, and Chinburg S.J. (1980). Carbonate sediment drifts in the northern Straits of Florida. AAPG Bulletin, 64, 1701–1717.

Mutti, E. (1992). Turbidite Sandstones. Agip Special Publication, Milan, Italy, p. 275.

Parsons, J.D., Whipple, K., Simoni. A. (2001). Experimental Study of the Grain-Flow, Fluid-Mud Transition in Debris Flows. [The Journal of Geology, 109, 427–447.

Phillips, C.J., Davies, T.R.H. (1991). Determining rheological parameters of debris flow material. Geomorphology, 4, 101-110.

Piper, D.J.W., Pirmez, C., Manley, P.L., Long, D., Flood, R.D., Normark, W.R., et al. (1997). Masstransport deposits of the Amazon Fan. In: Flood, R.D., Piper, D.J.W., Klaus, A., Peterson, L.C. (Eds.), Proceedings of the Ocean Drilling Program, Scientific Results, 155, pp. 109-143.·

Postma, G. (1986). Classification of sediment gravity-flow deposits based on flow conditions during sedimentation. Geology, 14, 291-294.

Prandtl, L. (1925). Bericht fiber Untersuchungen zur ausgebildeten Turbulenz. ZAMM, 5, 136–139.

Prandtl, L. (1926). Bericht fiber neuere Turbulenzforschung. In: Hydraulische Probleme, VDI-Verlag,Berlin, pp. 1–13.

Purkey, S.G., W.M. Smethie, G. Gebbie, A.L. Gordon, R.E. Sonnerup, M.J. Warner, and J.L. Bullister, (2018), A Synoptic View of the Ventilation and Circulation of Antarctic Bottom Water from Chlorofluorocarbons, *Annual Review of Marine Science*, 10, 503-527.

Rebesco M, Camerlenghi A, and Van Loon AJ (2008). Contourite research: A field in full development. In: Rebesco M and Camerlenghi A (eds.) Contourites, developments in sedimentology. vol. 60, pp. 3–10. Amsterdam: Elsevier.

Rebesco, M., Hernández-Molina, F.J., Van Rooij, D., Wåhlin, A., (2014). Contourites and associated sediments controlled by deep-water circulation processes: state-of-the-art and future considerations. Marine Geology, 352, 111-154.

Rodine, J.D., Johnson, A.M. (1976). The ability of debris, heavily freighted with coarse clastic material to flow on gentle slopes. Sedimentology, 23, 213-234.

Sanders, J.E. (1965). Primary sedimentary structures formed by turbidity currents and related resedimentation mechanisms. In: Middleton, G.V. (Ed.), Primary Sedimentary Structures and Their Hydrodynamic Interpretation, 12. SEPM Special Publication, Tulsa, OK, pp. 192-219.

Shanmugam, G. (1996). High-density turbidity currents: are they sandy debris flows? Journal of Sedimentary Research, 66, 2–10.

Shanmugam, G. (1997). The Bouma sequence and the turbidite mind set. Earth- Science Reviews, 42, 201–229.

Shanmugam, G. (2000). 50 years of the turbidite paradigm (1950s–1990s): deep-water processes and facies models—a critical perspective. Marine and Petroleum Geology, 17, 285–342.

Shanmugam, G. (2002). Ten turbidite myths. Earth-Science Reviews, 58, 311–341.

Shanmugam, G. (2003). Deep-marine tidal bottom currents and their reworked sands in modern and ancient submarine canyons. Marine and Petroleum Geology, 20, 471–491..

Shanmugam, G. (2006). Deep-water Processes and Facies Models, Implications for Sandstone Petroleum Reservoirs, vol. 5. Elsevier, Handbook of Petroleum Exploration and Production, Amsterdam, 476 p.

Shanmugam, G. (2012). New Perspectives on Deep-water Sandstones, Origin, Recognition, Initiation, and Reservoir Quality. In: Handbook of Petroleum Exploration and Production, vol. 9. Elsevier, Amsterdam, p. 524.

Shanmugam, G. (2013). Modern internal waves and internal tides along oceanic pycnoclines, challenges and implications for ancient deep-marine baroclinic sands. AAPG Bulletin, 97 (5), 767-811.

Shanmugam, G. (2015). The landslide problem. Journal of Palaeogeography, 4(2), 109-166.

Shanmugam, G. (2016a). The seismite problem. Journal of Palaeogeorapghy, 5(4), 318-362.

Shanmugam, G. (2016b). The contourite problem. In: R. Mazumder (Ed.), Sediment provenance, chapter 9, 183–254. Elsevier.

Shanmugam, G. (2017a). Global case studies of soft-sediment deformation structures (SSDS): Definitions, classifications, advances, origins, and problems. *Journal of Palaeogeorapghy*, 6(4), 251-320.

Shanmugam, G. (2017b). The fallacy of interpreting SSDS with different types of breccias as seismites amid the multifarious origins of earthquakes: implications. Journal of Palaeogeography, 6(1), 12-44.

Shanmugam, G. (2017c). Contourites: Physical oceanography, process sedimentology, and petroleum geology. *Petroleum Exploration and Development*, 44(2), 183-216..

Shanmugam, G. (2018a). The hyperpycnite problem. *Journal of Palaeogeography*, 7 (3), 197-238.

Shanmugam, G.. (2018b). A global satellite survey of density plumes at river mouths and at other environments: Plume configurations, external controls, and implications for deep-water sedimentation. *Petroleum Exploration and development*, 45 (4): 640-661.

Shanmugam, G. (2018c). Bioturbation and trace fossils in deep-water contourites, turbidites, and hyperpycnites: A cautionary note. In: Special Issue dedicated to George Devries Klein by the Journal of the Indian Association of Sedimentologists (JIAS). Journal of the Indian Association of Sedimentologists, Vol. 35, No. 2: 13-32.

Shanmugam, G. (2019a). Slides, Slumps, Debris Flows, Turbidity Currents, Hyperpycnal Flows, and Bottom Currents. In: Encyclopedia of Ocean Sciences (Third Edition) Volume 4, 228-257.

Shanmugam, G. (2019b}. Reply to discussions by Zavala (2019) and by Van Loon, Hüeneke, and Mulder (2019) on Shanmugam, G. (2018, Journal of Palaeogeography, 7 (3): 197-238): 'The hyperpycnite problem' Journal of Palaeogeography, 8 (3), 408-421.

Shanmugam, G. (2020). Mass transport, gravity flows, and bottom currents. Elsevier, 608 p.

Shanmugam, G., Benedict, G.L. (1978). Fine-grained carbonate debris flow, Ordovician basin margin, Southern Appalachians. J. Sedimentary Petrol. 48, 1233-1240.

Shanmugam, G., Spalding, T.D., Rofheart, D.H. (1993). Process sedimentology and reservoir quality of deep-marine bottom-

current reworked sands (sandy contourites): an example from the Gulf of Mexico. AAPG Bulletin, 77, 1241-1259.

Shanmugam, G., Lehtonen, L.R., Straume, T., Syversten, S.E., Hodgkinson, R.J., Skibeli, M. (1994). Slump and debris flow dominated upper slope facies in the Cretaceous of the Norwegian and Northern North Seas (61º-67 º N), implications for sand distribution. AAPG Bulletin, 78, 910-937

Shanmugam, G., Bloch, R.B., Mitchell, S.M., Beamish, G.W.J., Hodgkinson, R.J., Damuth, J.E., Straume, T., Syvertsen, S.E., Shields, K.E. (1995). Basin-floor fans in the North Sea, sequence stratigraphic models vs. sedimentary facies. AAPG Bulletin, 79, 477-512.

Shanmugam, G., Shrivastava, S.K., Das, B. (2009). Sandy debrites and tidalites of Pliocene reservoir sands in upper-slope canyon environments, Offshore Krishna-Godavari Basin (Iindia): Implications. J. Sedimentary Res. 79, 736-756.

Shepard, F.P., Dill, R.F. (1966). Submarine Canyons and Other Sea Valleys. Rand McNally & Co., Chicago, p. 381.

Shultz, A.W. (1984). Subaerial debris-flow deposition in the upper Paleozoic Cutler Formation, Western Colorado. J. Sedimentary Petrol. 54, 759-772.

Steel, E., A.R. Simms, J. Warrick, and Y. Yokoyama. 920160. Highstand shelf fans: The role of buoyancy reversal in the deposition of a new type of shelf sand body. GSA Bulletin, 128, 1717–1724.

Shipboard Scientific Party 919940. In: Mountain GS, Miller KG, and Blum P, et al. (eds.) Site 905, Proceedings of ocean drilling program, initial reports, College Station, Texas vol. 134,255–308. https://doi.org/10.2973/odp.proc.ir. 150.109. 1994.

Stommel, H. 919580. The abyssal circulation. Deep-Sea Research, 5, 80–82.

Stow, D.A.V. 91985). Deep-sea clastics, where are we and where are we going? In: Brenchly, P.J., Williams, P.J. (Eds.), ,Sedimentology, Recent Developments and Applied Aspects. Published for the Geological Society by Blackwell Scientific Publications, Oxford, UK, pp. 67-94.

Stow, D.A.V., Shanmugam, G. (1980). Sequence of structures in fine-grained turbidites, comparison of recent deep-sea and ancient flysch sediments. Sedimentary Geology, 25, 23-42.

Stow, D. A. V., Faugères, J. C. (2008). Contourite facies and the facies model. In: Rebesco, M., Camerlenghi, A. (eds.), Contourites. Elsevier, Amsterdam, Developments in Sedimentology 60, pp. 223–256. Chapter 13.

Stow, D.A.V., Hunter S, Wilkinson D, and Hernández-Molina F.J. (2008). The nature of contourite deposition. In: Rebesco M and Camerlenghi A (eds.) Contourites. Developments in sedimentology. vol. 60, pp. 143–156. Amsterdam: Elsevier. (Chapter 9)

Stow, D.A.V. Brackenridge R Hernandez-Molina FJ. (2011). Contourite sheet sands: new deepwater exploration target. Abstract American Association of Petroleum Geologists Annual Conference, Houston 2011.

Su, D.C., Sun, A.P. (2012). Typical earthquake-induced soft sediment deformation structures in the Mesoproterozoic Wumishan Formation, Yongding River Valley, Beijing, China and interpreted earthquake frequency. Journal of Palaeogeography, 1, 71e89.

Talley, L.D. (2013). Closure of the global overturning circulation through the Indian, Pacific, and Southern Oceans: schematics and transports. Oceanography, 26 (1), 80-97.

Talling, P. J. (2013).Hybrid submarine fl ows comprising turbidity current and cohesive debris fl ow: Deposits, theoretical and experimental analyses, and generalized models. Geosphere, 3) 9 (3), 460–488.

Teale, T. Young, J.R. (1987). Isolated olistoliths from the Longobucco Basin Calabria, S. Italy. In: Leggett, J.K. and Zuffa, G.G. (eds.) Advances in marine clastic sedimentology, pp. 75–88. London, UK: Graham & Trotman.

Van Loon, A. J. (Tom), Hüeneke, H., and Mulder, T. (2019). The hyperpycnite problem: Comment. *Journal of Palaeogeography*, 8

Viana, A.R. (2008). Economic relevance of contourites. In: Rebesco M and Camerlenghi A (eds.) Contourites: Developments in sedimentology. vol. 60, pp. 493–510. Amsterdam: Elsevier. (Chapter 23).

Walker, R.G. (1965). The origin and significance of the internal sedimentary structures of turbidites. Proceedings of the Yorkshire Geological Society, 35, 1–32.

Wallis, G.B. (1969). One-dimensional Two-phase Flow. McGraw-Hill, New York, p. 408.

Wang, H., N. Bi, Y. Wang, Y. Saito, and Z. Yang. (2010). Tide-modulated hyperpycnal flows off the Huanghe (Yellow River) Mouth, China. Earth Surface Processes and Landforms, 35 (11), 1315–1329.

Warrick, J.A., A.R. Simms, A. Ritchie, E. Steel, P. Dartnell, J.E. Conrad, and D.P. Finlayson. (2013). Hyperpycnal plumederived fans in the Santa Barbara channel, California. Geophysical Research Letters, 40, 2081–2086.

Wright, L.D., Nittrouer CA. (1995). Dispersal of river sediments in coastal seas: six contrasting cases. Estuaries, 18(3), 494–508.

Wust, G. (1936). Schichtung und Zikulation des Atlantischen Ozeans. Das Bodenwasser und die Stratosphare: Duetschen Atlantischen Expedition. Tiefsee.Geologische Rundschhau, 47, 187–195.

Zavala, C. (2019). The new knowledge is written on sedimentary rocks- a comment on Shanmugam's paper "The hyperpycnite problem". *Jour. of Palaeogeography*, 8, 306-313.

Zavala, C., (2020). Hyperpycnal (over density) flows and deposits. Journal of Palaeogeography (2020) 9:17. https://doi.org/10.1186/s42501-020-00065-x

Zavala, C., and M. Arcuri. (2016). Intrabasinal and extrabasinal turbidites: Origin and distinctive characteristics. Sedimentary Geology, 337, 36–54.

Zenk, W. (2008). Abyssal and contour currents. In: Rebesco M and Camerlenghi A (eds.) Contourites: Developments in sedimentology. vol. 60, pp. 37–57. Amsterdam: Elsevier. (Chapter 4).

Zou, C., Wang, L., Li, Y., Tao, S., and Hou, L. (2012). Deep-lacustrine transformation of sandy debrites into turbidites, pper Triassic, Central China. Sedimentary Geology, 265 266, 14.